JOURNAL OF
APPLIED ANIMAL SCIENCE

ISSN 1906-2257 VOL.15 NO.1 JANUARY-JUNE 2022

"Journal of Applied Animal Science" (JAAS)

Scope of the Journal

The philosophy of the Faculty of Veterinary Science, Mahidol University, is *"One Health"*, i.e., to interweave the disciplines of veterinary sciences with medical sciences for extreme advantages to human, animals and environment. The *Journal of Applied Animal Science (JAAS)*, is a peered review journal which published 2 numbers (January-June, July-December) a year by Faculty of Veterinary Science, Mahidol University, accepts manuscripts presenting information for publication with this philosophy in mind. Articles published in *JAAS* include a broad range of research topics in veterinary science, animal science, animal husbandry, animal production and fundamental aspects of genetics, nutrition, physiology, and preparation and utilization of animal products. Articles typically report research with cattle, companion animals, goats, horses, pigs, and sheep; however, studies involving other farm animals, aquatic and wildlife species, and laboratory animal species that address fundamental questions related to livestock and companion animal biology will be considered for publication.

Journal Management

คณะสัตวแพทยศาสตร์ มหาวิทยาลัยมหิดล

999 ถนนพุทธมณฑล สาย 4 ตำบลศาลายา อำเภอพุทธมณฑล จังหวัดนครปฐม 73170

โทร. 0-2441-5242 ต่อ 1308 โทรสาร 0-2441-0937

Website http://www.vs.mahidol.ac.th/jaas Editor-in-Chief: Assoc.Prof. Dr.Tanasak Changbunjong, E-mail address: editor.jaas2020@gmail.com

Journal manager: Natcha Kaewkrajang

จัดพิมพ์โดย :

ห้างหุ้นส่วนสามัญนิติบุคคล ปอยท์ กราฟิค

177/2 ซอยจรัญสนิทวงศ์ 11 ถนนจรัญสนิทวงศ์ แขวงวัดท่าพระ เขตบางกอกใหญ่ กรุงเทพฯ 10600

โทร. 08-1826-5455 E-mail address: pointswift@yahoo.com

"Journal of Applied Animal Science" (JAAS)

สารจากคณบดี

Journal of Applied Animal Science Vol. 15 No. 1 Jan-Jun 2022 นี้ เป็นพัฒนาการภายใต้การนำทีมของบรรณาธิการวารสาร รศ.ดร.น.สพ.ธนศักดิ์ ช่างบรรจง ที่ได้เปลี่ยนรูปแบบการ submit บทความผ่านทางระบบออนไลน์ฐานข้อมูลวารสารอิเล็กทรอนิกส์กลางของประเทศไทย (Thai Journals Online (ThaiJO)) ที่อยู่บนระบบเดียวกันกับระบบ Online Journal System (OJS) ซึ่งพัฒนาโดย Public Knowledge Project (PKP) ซึ่งก้าวย่างนี้ เป็นก้าวที่สำคัญที่เปิดโอกาสให้นักวิจัย นักวิชาการ สัตวแพทย์ส่งผลงานได้สะดวกและเป็นระบบมากยิ่งขึ้น ดังปรากฏในเนื้อหาฉบับนี้ทั้งในรูปแบบ original article และ case report ที่มีความหลากหลาย ซึ่งเชื่อได้ว่าเหล่านี้ล้วนเป็นองค์ความรู้ที่สำคัญซึ่งเป็นพื้นฐานของความคิดริเริ่ม ที่เป็นองค์ประกอบขั้นพื้นฐานของการสร้างนวัตกรรม

ขอขอบคุณบรรณาธิการวารสาร รศ.ดร.น.สพ.ธนศักดิ์ ช่างบรรจง และผู้รับผิดชอบงานวารสารทุกท่าน ตลอดจนนักวิชาการเจ้าของบทความ ที่ได้สละเวลาอันมีค่าจัดทำเล่มวารสาร ประสานงานและอำนวยความสะดวกกับผู้เขียนบทความตั้งแต่เริ่มต้นจนแล้วเสร็จ และขอเป็นกำลังใจให้ผู้รับผิดชอบ Journal of Applied Animal Science สามารถผลิตผลงานและบรรลุผลตามวัตถุประสงค์ทุกประการ

รองศาสตราจารย์ ดร.สัตวแพทย์หญิงวลาสินี ศักดิ์คำดวง
คณบดีคณะสัตวแพทยศาสตร์
มหาวิทยาลัยมหิดล

"Journal of Applied Animal Science" (JAAS)

ปีที่ 15 ฉบับที่ 1 มกราคม-มิถุนายน 2565 Vol. 15 No. 1 January-June 2022

สารบัญ

คำแนะนำสำหรับผู้แต่ง

"Journal of Applied Animal Science" (JAAS)

วารสารสัตวศาสตร์ประยุกต์เป็นวารสารวิชาการราย 6 เดือน (2 ฉบับต่อปี เดือนมกราคม-มิถุนายน และเดือนกรกฎาคม-ธันวาคม) ของคณะสัตวแพทยศาสตร์ มหาวิทยาลัยมหิดล เผยแพร่ผลงานวิจัยครอบคลุมสหสาขาวิชาทั้งสัตวแพทยศาสตร์ และสัตวศาสตร์ ตั้งแต่พื้นฐานถึงระดับโมเลกุล รวมถึงรายงานทางคลินิก บทความที่ได้รับการตีพิมพ์ในวารสารต้องผ่านการประเมินโดยผู้ทรงคุณวุฒิอย่างน้อย 3 ท่าน ในรูปแบบ double-blind peer review

ผู้สนใจส่งบทความเพื่อตีพิมพ์ในวารสารสัตวศาสตร์ประยุกต์กรุณาปฏิบัติตามข้อแนะนำและส่งพร้อมจดหมายนำ

1. ประเภทบทความ ที่รับพิจารณาได้แก่ รายงานการวิจัย รายงานฉบับย่อ บทความปริทัศน์และรายงานทางคลินิกเขียนด้วยภาษาไทยหรือภาษาอังกฤษ แต่บทคัดย่อต้องมีทั้งภาษาไทยและภาษาอังกฤษ

2. การส่ง ส่งต้นฉบับพร้อมสำเนา 4 ชุด และไฟล์ดิจิตอลทางไปรษณีย์ ไฟล์ดิจิตอลต้องสร้างด้วยโปรแกรม MS-Word หรือซอฟต์แวร์ที่ใช้แทนกันได้ อาจส่งต้นฉบับผ่านอีเมลโดยไม่มีสำเนาได้

3. รูปแบบ ขนาดกระดาษเอ 4 พิมพ์หน้าเดียว เว้นระยะ 1 บรรทัด ขอบกระดาษ 2.54 ซม. (1 นิ้ว) ฟอนต์ Angsana New หรือ TH SarabunPSK 16 พอยต์

4. ส่วนประกอบ รายงานการวิจัยต้องประกอบด้วยหน้าแรก (ได้แก่ ชื่อเรื่อง ชื่อผู้แต่ง สถานที่ทำงานและที่อยู่ชื่อผู้แต่งหลักพร้อมที่อยู่ที่ติดต่อได้และอีเมล พิมพ์ทั้งภาษาไทยและภาษาอังกฤษ) บทคัดย่อ (สั้นกระชับได้ใจความและคำสำคัญ 3-4 คำ) บทนำ อุปกรณ์และวิธีการ ผลการวิจัย วิจารณ์ กิตติกรรมประกาศและเอกสารอ้างอิง

ก. รายงานฉบับย่อและรายงานทางคลินิก อาจเขียนโดยไม่แยกหัวข้อ หรืออาจรวมส่วนผลการวิจัยและวิจารณ์เป็นหัวข้อเดียว

ข. บทความปริทัศน์ ควรเริ่มด้วยบทนำ แล้วบรรยายโดยแยกตามหัวข้อที่ต้องการนำเสนอ พร้อมบทสรุป

5. ตาราง-รูปภาพ ตารางและรูปภาพให้แทรกไว้ท้ายสุดของบทความ คำบรรยายตารางพิมพ์ด้านบน คำบรรยายรูปภาพพิมพ์ใต้ภาพ และมีหมายเลขอาระบิกกำกับตามลำดับการอ้างถึง ตารางควรเข้าใจได้ง่าย ให้ส่งรูปภาพความละเอียดสูงแยกต่างหากมาพร้อมด้วย

6. การอ้างอิง ผู้แต่งต้องปฏิบัติตามรูปแบบการอ้างอิงของวารสาร การอ้างอิงในเนื้อหาใช้ระบบนาม-ปี เช่น (คัมภีร์ กอธีระกุล และคณะ 2530) หรือ คัมภีร์ กอธีระกุล และคณะ (2530) การเขียนรายการเอกสารอ้างอิงให้เขียนไว้หลังกิตติกรรมประกาศ โดยพิมพ์เอกสารภาษาไทยก่อนแล้วตามด้วยเอกสารภาษาอังกฤษ สำหรับการเขียนเอกสารอ้างอิงภาษาอังกฤษให้ดูจากส่วนแนะนำภาษาอังกฤษ

คัมภีร์ กอธีระกุล, เทิด เทศประทีป, วรา พานิชเกรียงไกร, โสมทัต วงศ์สว่าง, วราภรณ์ แซ่ลี้, สมศักดิ์ ภัคีศิริภรณ์. การสำรวจพบเชื้อ *อี.โคไล* ซีโรไทป์ K88 จากลูกสุกรวัยดูดนมและหลังหย่านม. เวชชสารสัตวแพทย์. 2530; 17(1): 21-7.

7. ชื่อวิทยาศาสตร์ ให้พิมพ์เป็นภาษาอังกฤษตามประมวลนามศัพท์สากลและทำให้เด่นแตกต่างจากเนื้อหา

8. การถอดคำไทยเป็นภาษาอังกฤษ ใช้หลักเกณฑ์การถอดอักษรไทยเป็นอักษรโรมันแบบถ่ายเสียงของราชบัณฑิตยสถาน

9. อักษรย่อและสัญลักษณ์ หากเป็นที่รับรู้โดยทั่วกันอนุโลมให้ใช้ได้โดยไม่ต้องพิมพ์ตัวเต็มก่อน

สำหรับรายละเอียดเพิ่มเติมและแม่แบบต้นฉบับ ให้ไปที่เว็บไซต์ของวารสาร https://he02.tci-thaijo.org/index.php/jaas_muvs

อีเมลบรรณาธิการวารสาร editor.jaas2020@gmail.com

ที่อยู่ คณะสัตวแพทยศาสตร์ มหาวิทยาลัยมหิดล 999 ถนนพุทธมณฑล สาย 4 ตำบลศาลายา อำเภอพุทธมณฑล จังหวัดนครปฐม 73170

Instructions to Authors

"Journal of Applied Animal Science" (JAAS)

Journal of Applied Animal Science is a peer-review journal (2 issues/year; January-June and July-December) which publishes papers that report on original research covering broadly interdisciplinary of veterinary and animal sciences with results of more than local regard. *JAAS* invite and welcome submissions on existing new research from basic to molecular. Articles published under our journal are double-blind peer reviewed by at least 3 reviewers.

The author should follow the instructions below for manuscript preparation and submit with covering letter.

1. Categories: *JAAS* accepts varieties of article, including research articles, short communications, reviews and also clinical reports.

2. Language: English articles are preferable; however, both Thai and English manuscripts are acceptable, with Thai and English abstracts.

3. Submission: Submission via email is our most preferable way. However, submission of the manuscript is acceptable by either paper (4 copies) or digital format (email). Finally, digital format must be submitted. The submission file is in MS-Word format or compatible software.

4. Format: The manuscript should be used A4 size with margin of 2.54 cm (1 in), double spacing and indentions by using tabs. Times New Roman font 12 points is favored for English and Angsana New or TH SarabunPSK 16 points is desirous for Thai.

5. Components: The research manuscripts should have sequential components as title page, abstract and 3-4 keywords, introduction, materials and methods, results, discussion, conclusion, acknowledgements and references. Title page, in both Thai and English, includes title, author(s) and affiliation(s) for each author. Corresponding author must provide full contact address and email.

a. Short communications or clinical reports: These could be written as no sections, combination of results and discussion or introduction and followed by several presentation sections.

b. Reviews: The manuscript should start with introduction and followed by demonstration sections and conclusion.

6. Tables-Figures: Tables and figures must be numbered by using Arabic numbers. The caption must be written on the top of table or the bottom of figure. Tables and figures should be put at the end of article. All tables should be understandable by itself. All figures with high quality should be prepared in black and white as separate files.

7. References: Authors must be careful for the reference formats of both in-text citations and bibliography. In-text citations use author(s)-year in parentheses, the proper format is (Smith 2008; Kennedy and Smith 2009; John et al., 2010a, 2010b) or Smith (2008).Two authors use "and" in between. Using "et al.," when there are more than 2 authors. Multiple citations in a sentence must be in chronological order first, then alphabetical order. Bibliography should be in the last part of article and arranged alphabetically by authors or title. List first 6 authors and followed by "et al." when there are more than 6 authors. The title is followed the last author. Abbreviated journals are according to the conventional ISO abbreviations used by PubMed. One-word journal title must be spelled out. Year of publication, volume, issue in parentheses, and begin and end pages. These are examples of bibliography.

Barker K. At the Bench: A laboratory navigator. New York: Cold Spring Harbor Laboratory Press; 1998.

Fairbrother JM, Gyles CL. Escherichiacoliinfections. In: Straw BE, Zimmerman JJ, D'Allaire S, Taylor DJ, editors. Diseases of swine. 9th ed. Iowa: Blackwell Publishing; 2006. p. 639-74.

Laohasinnarong D, Kaeoket K, Prasitphon B. Estrus synchronization in gilts with altrenogest by different given time. Proceedings of the 19th IPVS Congress. Copenhagen, Denmark: Narayana Press; 2006. p. 118.

Meng X-J, Purcell RH, Halbur PG, Lehman JR, Webb DM, Tsareva TS, et al. A novel virus in swine is closely related to the human hepatitis E virus. Proc Natl Acad Sci. 1997;94(18):9860-5.

WHO media centre. African trypanosomiasis (sleeping sickness) [Internet]. WHO. 2010 [cited 2011 Oct 29]. Available from: http://www.who.int/mediacentre/factsheets/fs259/en/.

8. Scientific terms should use the update and follow the International Code of Nomenclature, written by emphasis.

9. Standard abbreviations and symbols are acceptable without definition.

Please visit *JAAS* website for more information and manuscript template, https://he02.tci-thaijo.org/index.php/jaas_muvs

Editor-in-Chief email: editor.jaas2020@gmail.com

Address: Faculty of Veterinary Science, Mahidol University, 999 Phuttamonthon Sai 4, Salaya, Phuttamonthon, Nakornphatom 73170 Thailand.

Editor Note

สวัสดีครับท่านผู้อ่านและสมาชิกวารสาร Journal of Applied Animal Science (JAAS) ทุกท่าน ก่อนอื่นต้องขอแสดงความยินดีที่วารสารของเราได้เข้าสู่ระบบฐานข้อมูลวารสารอิเล็กทรอนิกส์กลางของประเทศไทย (Thai Journals Online (ThaiJO)) ซึ่งวารสารฉบับนี้ (ปีที่ 15 ฉบับที่ 1 ปี พ.ศ. 2565) นับว่าเป็นวารสารฉบับแรกที่ผู้แต่งได้ส่งบทความออนไลน์ผ่านระบบ ThaiJO อย่างเต็มรูปแบบ และผู้อ่านสามารถติดตามบทความอัพเดตได้ที่เวปไซต์ของวารสาร https://he02.tci-thaijo.org/index.php/jaas_muvs

สำหรับวารสารฉบับนี้ประกอบด้วยบทความที่น่าสนใจได้แก่ บทความวิจัย 3 เรื่อง "การเปลี่ยนแปลงทางพยาธิสภาพระดับมหกายวิภาคภายหลังการตายของหนูแรทภายใต้สภาพแวดล้อมห้องเลี้ยงสัตว์ทดลอง" "การศึกษาเบื้องต้นในหลอดทดลองเกี่ยวกับผลของสายพันธุ์ของเชื้อไวรัสซิกาต่อคุณภาพอสุจิสุกร" และ "แบบจำลองพลวัตการแพร่กระจายของกาฬโรคแอฟริกาในม้าในการระบาดครั้งแรกในประเทศไทย" รายงานกรณีศึกษา 1 เรื่อง "โรคเส้นเลือดลัดข้ามตับในแมว"

ทั้งนี้ทางวารสารขอเชิญชวนท่านผู้อ่านหรือผู้ที่สนใจร่วมส่งบทความทั้งในรูปแบบของบทความวิจัย (Research article) บทความปริทัศน์ (Review article) บทความวิจัยสื่อสารอย่างสั้น (Short communication) หรือรายงานกรณีศึกษา (Case report) เพื่อตีพิมพ์ในวารสาร JAAS โดยท่านสามารถส่งบทความได้ที่ https://he02.tci-thaijo.org/index.php/jaas_muvs/about/submissions หรือสามารถติดต่อสอบถามรายละเอียดเพิ่มเติมได้ที่อีเมล editor.jaas2020@gmail.com

รองศาสตราจารย์ ดร.นายสัตวแพทย์ธนศักดิ์ ช่างบรรจง

บรรณาธิการ (Editor-in-Chief)

MUVETO

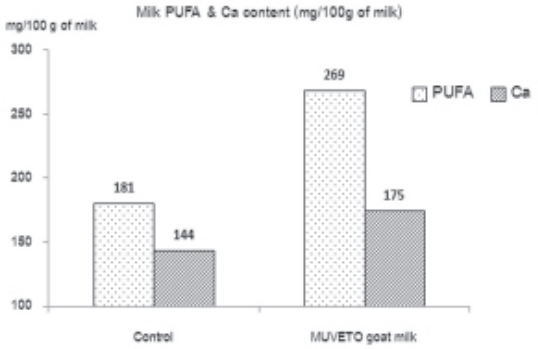

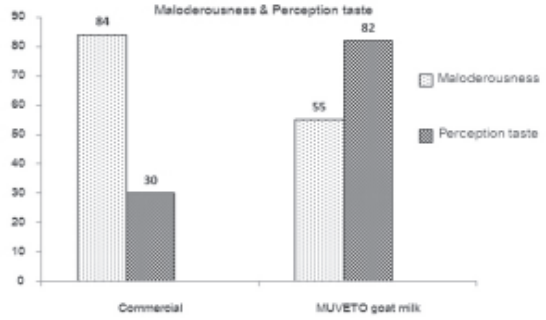

Functional goat milk: Naturally high PUFA,Ca and maloderousness

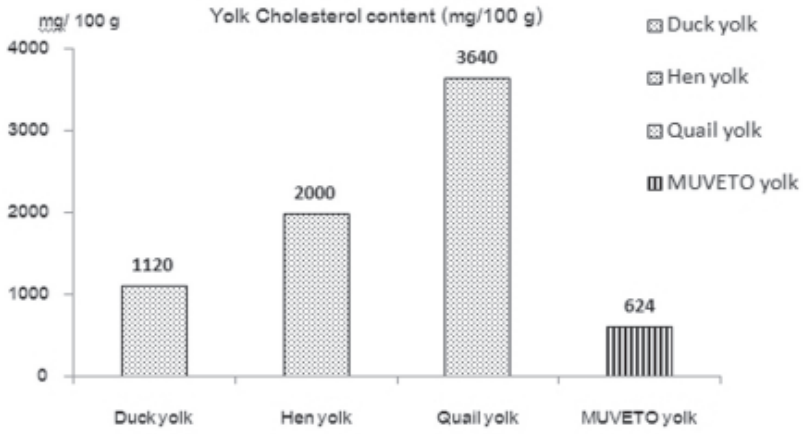

Functional egg: Low cholesterol

Distributed by : Faculty of Veterinary Science, Mahidol University
999 Phutthamonthon Sai 4 Road, Salaya, Phutthamonthon,
Nakhonpathom, 73170, Thailand. Tel. 02-4410933.

Research Articles

Postmortem Macroscopic Changes in Rats under Rat House Conditions

Panida Butrat Masupa Boonmayaphan*

National Laboratory Animal Center, Mahidol University
999 Phuttamonthon 4 Rd., Salaya, Phuthamonthon, Nakhon Pathom, Thailand 73170

***Corresponding author, E-mail address: masupa.jat@mahidol.edu**

Received: 1 April 2022; Revised: 9 June 2022; Accepted: 17 June 2022

Abstract

This research aims to study the postmortem macroscopic changes in rat under rat house conditions. The results of this study will help researchers or veterinarians determine causes of animal death in colonized animals and research studies. This study used thirty-six healthy rats with body weights from 190 to 230 g. Throughout this study, the Animals were housed under controlled environmental conditions of the National Laboratory Animal Center, Mahidol University (22 ± 3 °C, 30 - 70% relative humidity). After euthanasia, animals were maintained in the ventral recumbency position in their cages. Macroscopic changes in the laboratory rat carcasses were observed. Ocular changes were evaluated at 0, 1, 2, 4, 6, 8, 12, 18, 24, 36, and 48 h postmortem. Gross appearances were investigated at 4, 8, 12, 24, and 48 h postmortem in accordance with necropsy examination of internal organs. The results showed that rat carcasses had different characteristics at different times. Ocular changes began immediately 0-4 h after euthanasia, and progressed to total sunken eyes at 24 h. Skin discoloration appeared 8 h after death. Internal findings from livor mortis observations of the internal organs showed that lividity varied from red to purple and became darker with the increasing postmortem interval, especially in the liver and spleen. Moreover, the decomposition of internal organs disintegrated at different rates. The pancreas, gastrointestinal tract, liver, and thyroid showed autolysis early in the postmortem interval (PMI) and increased their severity with time. At 48 h, necropsy revealed that the internal organs were vigorously twisted, collapsed, softened, liquefied, and dissolved. Our results suggest that postmortem ocular changes and macroscopic changes are useful for differentiating postmortem changes from antemortem and can aid in PMI estimation in laboratory rats, which will be beneficial for death investigations concerning laboratory rats.

Keywords: Postmortem changes, Postmortem interval, Postmortem macroscopic changes, Ocular changes

การเปลี่ยนแปลงทางพยาธิสภาพระดับมหกายวิภาคภายหลังการตายของหนูแรทภายใต้สภาพแวดล้อมห้องเลี้ยงสัตว์ทดลอง

พนิดา บุตรรัตน์ มาศสุภา บุญมาญะพันธ*

ศูนย์สัตว์ทดลองแห่งชาติ มหาวิทยาลัยมหิดล
999 ถ.พุทธมณฑล สาย 4 ศาลายา จ.นครปฐม 73170

*ผู้รับผิดชอบบทความ E-mail address: masupa.jat@mahidol.edu

Received: 1 April 2022; Revised: 9 June 2022; Accepted: 17 June 2022

บทคัดย่อ

งานวิจัยนี้มีวัตถุประสงค์เพื่อศึกษาการเปลี่ยนแปลงทางพยาธิสภาพระดับมหกายวิภาคภายหลังการตายของหนูแรทภายใต้สภาพแวดล้อมห้องเลี้ยงสัตว์ทดลอง ซึ่งการศึกษานี้จะเป็นประโยชน์แก่สัตวแพทย์และนักวิจัย ในการผ่าชันสูตรซากของหนูแรทในโคโลนีหรืองานวิจัย เพื่อช่วยในการวินิจฉัยหาสาเหตุการตายของสัตว์ การศึกษานี้ใช้หนูแรทสุขภาพดี น้ำหนัก 190-230 กรัม จำนวน 36 ตัว สัตว์แต่ละตัวถูกแยกเลี้ยงเดี่ยวในกรงภายใต้ห้องเลี้ยงสัตว์ทดลองของศูนย์สัตว์ทดลองแห่งชาติ มหาวิทยาลัยมหิดล ที่มีการควบคุมสภาพแวดล้อม หลังจากการุณยฆาตนำสัตว์ไปไว้ในกรงเดิมในท่านอนคว่ำ (ventral recumbency) การศึกษานี้มุ่งเน้นศึกษาในเรื่องการเปลี่ยนแปลงทางพยาธิสภาพระดับมหกายวิภาคของหนูแรท ประเมิน ocular changes ที่ 0, 1, 2, 4, 6, 8, 12, 18, 24, 36 และ 48 ชั่วโมงภายหลังการตาย และการเปลี่ยนแปลงทางพยาธิสภาพจากการสังเกตและการผ่าชันสูตรซากอวัยวะภายใน ที่ 4, 8, 12, 24 และ 48 ชั่วโมงภายหลังการตาย จากการศึกษาแสดงให้เห็นว่าซากมีการเปลี่ยนแปลงแตกต่างกันในแต่ละช่วงเวลาที่ต่างกัน การเปลี่ยนแปลงของตาพบได้ที่ชั่วโมงที่ 0-4 ต่อเนื่องไปจนพบ sunken eyes ที่ 24 ชั่วโมงภายหลังการตาย การเปลี่ยนแปลงภายนอกร่างกายสัตว์เริ่มพบ skin discoloration ที่ 8 ชั่วโมงภายหลังการตาย ส่วนการเปลี่ยนแปลงภายในร่างกายสัตว์จากการเกิด livor mortis ของอวัยวะภายในแสดงให้เห็นระดับ lividity สีแดงถึงม่วง และเข้มขึ้นตามเวลาที่เพิ่มขึ้นโดยแตกต่างกันในสัตว์แต่ละตัว ซึ่งจะสามารถเห็นได้ชัดเจนในตับและม้าม สำหรับ decomposition ของอวัยวะภายใน พบในระดับที่แตกต่างกันไป ผลการศึกษานี้พบว่า ตับอ่อน ระบบทางเดินอาหาร ตับ และไทรอยด์ จะพบการเกิด autolysis เป็นอวัยวะแรกๆ และมีระดับที่รุนแรงขึ้นตามเวลาที่เพิ่มขึ้น การผ่าชันสูตรซากในชั่วโมงที่ 48 ภายหลังการตาย พบว่าอวัยวะภายในเกิดการ twisted, collapsed, soften, liquefied และ dissolution อย่างรุนแรง การศึกษาส่งผลให้เห็นว่า postmortem ocular change และ macroscopic change สามารถนำมาใช้เป็นข้อมูลพื้นฐานเพื่อเปรียบเทียบแยกแยะระหว่าง postmortem และ antemortem อีกทั้งยังช่วยในการประมาณหรือเทียบเคียงหาระยะเวลาการตายของหนูแรทได้ ซึ่งจะเป็นประโยชน์ในการช่วยวิเคราะห์หาสาเหตุการตายของหนูแรทในห้องเลี้ยงสัตว์ทดลองได้

คำสำคัญ : การเปลี่ยนแปลงภายหลังการตาย การประมาณระยะเวลาการตาย การเปลี่ยนแปลงพยาธิสภาพระดับมหกายวิภาค การเปลี่ยนแปลงของตาภายหลังการตาย

Journal of Applied Animal Science 2022; 15(1): 9-22.

Introduction

Immediately after death, postmortem changes will begin to develop. These changes include algor mortis, rigor mortis, livor mortis and decomposition (Merck 2013). Understanding general postmortem changes can help to indicate changes of body before (antemortem) and after death. Therefore, estimating the postmortem interval (PMI) is important because it contributes to determining the time frame during which the death occurred. Moreover, postmortem change studies and PMI analysis are a tools used to investigate the cause of death in humans, animals, and including laboratory animals.

Postmortem changes that occur after death results from complex physicochemical and environmental processes. These are affected by factors within the internal body and external factors. Internal factors affect postmortem changes, primarily including the body's surface area, body mass, body fat, open injuries, sepsis, and infection. While external factors hasten the rate of postmortem changes, such as the environment of the death scene and the storage of the body after death (Megyesi et al., 2005; Sutherland et al., 2013; Lowe et al., 2013).

Considerable research has been done to establish reliable and accurate time of death estimation methods in humans. Therefore, the estimated time of death can be used in law enforcement to solve death-related criminal cases. Since there is a significant amount of information about postmortem changes in humans, most animal studies have applied from human forensic. In addition, contemporary veterinary forensic medicine emphasizes PMI refining as one of the key challenges (Munro and Munro 2013).

In laboratory animals, it is necessary to determine or predict the cause of death. Such data would be helpful for research analysis and disease investigations in animal colonies. Furthermore, it is imperative to learn about postmortem macroscopic changes as it can help to differentiate postmortem from antemortem changes. Similarly, numerous methods have been proposed for the determination of PMI. Literature relating to early PMI estimation has continually adapted techniques, mainly focusing on algor mortis and rigor mortis. In rodents, the study by Dwi et al. (2017) showed an algor mortis pattern of rats at 0 to 22 h under ambient room and condition room. In addition, published data exist regarding the process of evolution and resolution of rigor mortis in rats, rigor was evaluated for each joint in time points (Krompecher 2016).

A macroscopic change is one of the essential tools. Morphologic changes begin immediately after death and continue over a prolonged period at different rates in different organs. Generally, visible changes on a gross level consist of discoloration, livor mortis, a sequence of decomposition (Brooks 2016) etc. For postmortem gross change, limited information is available on wildlife and companion animal species. One studies by Erlandsson and Munro (2007) on beagles showed the external and internal gross pathology observation at various time points after death. Some authors refer to the forensics of livestock, but studies on laboratory animals are limited or lacking in terms of data.

Nonetheless, a few studies have evaluated postmortem ocular change by macroscopic examination methods, such as a study on postmortem eye changes on corneal opacity and eye sinking in rodents to estimate the PMI (Capas-Peneda et al., 2016). Even though countless studies have investigated human postmortem changes and forensics, only a few of research have been conducted concerning postmortem changes and estimation of PMI in animals, especially laboratory animals. Understanding

postmortem changes corresponding to their PMI in laboratory animals can help researchers or veterinarians determine the cause of animal death in colonized animals and research studies. Thus, the objectives of this study is to evaluate postmortem changes at different death intervals. The observations included ocular, gross appearances, and internal organs. The results will be collected and developed as database of general postmortem changes, plus to estimate PMI in the laboratory animal house facility.

Materials and Methods

Animal

The study protocol was approved by National Laboratory Animal Center Animal Care and Use Committee (protocol number RA2021-17).

This study was carried out on 36 healthy Rattus norvegicus (Wistar rat). The Rats were divided into postmortem ocular change evaluation and gross change evaluation. The Animals were obtained from the Animal Production Office of National Laboratory Animal Center, Mahidol University. The animals were quarantined for a day and housed individually in open-topped cages with stainless steel wire-bar and solid bottom. Physical enrichment was provided while the rats were individually housed, including ribbon water hyacinth and PVC pipe. The cages contained mixed bedding of corn cobs and water hyacinth. Food and hyper chlorinated water (5-7 ppm.) were provided ad libitum. The housing conditions were controlled at a temperature of 22 ± 3 ^{o}C, with relative humidity (30-70 %) and ventilation rate >10 ACH, respectively, according to the Guide for the Care and Use of Laboratory Animals, Eight Edition. The animals were exposed to 12:12 hours of a light-dark cycle during this study. For the euthanasia method, rats were administrated 250 mg/kg of thiopental sodium intraperitoneally. After death was confirmed, the carcass was raised in ventral recumbency in their cages.

Postmortem ocular change evaluation

Sixteen rats (8 of each gender) were used in this study; their body weight ranged from 200 to 230 g. After the animals were euthanized, ocular changes were evaluated by macroscopic examination at 0, 1, 2, 4, 6, 8, 12, 18, 24, 36, and 48 h. The eyes were observed and given a score from 0 to 4, according to Table 1. The data were reported as the sample mean ± standard deviation (mean ± SD)

Table 1. Classification for postmortem ocular changes (Capas-Peneda et al., 2016).

Score	Ocular changes
0	Normal
1	Mild Corneal Opacity
2	Total Corneal Opacity
3	Mild Eye Sinking
4	Total Eye Sinking

Postmortem gross change evaluation

Twenty rats (10 of each gender) were used; the animals' body weight range from 190 - 230 g. Gross appearances were evaluated by observing general changes in the eyes and skin. Moreover, a necropsy was performed to study livor mortis, decomposition, displacement, and alterations of the internal organs. The animals were evaluated at 4, 8, 12, 24, and 48 h (four animals per time).

Results

Under the laboratory animal room conditions with normal temperature and relative humidity for the rat house facility, the results indicated that macroscopic changes had occurred at each time point and showed similar appearances in every animal within the same group; the discussion is given below.

Postmortem ocular changes

Ocular mucous membrane changed from pale to purple approximately 0 - 4 h after euthanasia. Mild corneal opacity began at 4 h postmortem observations, and complete total corneal opacity started at 6 h postmortem in some rats. The mild sinking of eyeball occurred during 12 - 18 h in all animals and evolved to total sinking about 24 h postmortem (Table 2).

Table 2. Classification for postmortem ocular changes in rats (n=16).

Ocular changes score		Time postmortem (h)
0 Normal		0 - 2
1 Mild Corneal Opacity	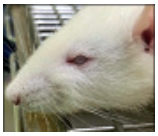	Start 4
2 Total Corneal Opacity		Start 6
3 Mild Eye Sinking		12 - 18
4 Total Eye Sinking	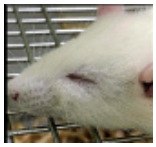	Start 24

Postmortem gross changes

External findings

Discoloration or color change of the skin and soft tissue was found in all animals of the same group. This study found dark red discoloration in the skin, nails, scrotum skin, and gums at approximately 12 h postmortem. The tip of the tongue became darkened, dry, and hard in appearance after 48 h postmortem. Eight hours after death, the caudal abdomen developed dark red to green discoloration. Within 12 h postmortem, dark green/purple discoloration was observed in all rats (Figure 2).

Internal findings

Livor mortis of the internal organs first appeared approximately 4 to 8 h postmortem. Lungs appeared dark purple area at 4 h, and diffuse congestion in all lobes was revealed at 12 h postmortem, while severe congestion was seen in all animals after 48 h (Figure 3). The thymus had mild congestion (reddish-purple spots) at the 8 h necropsy time, and severe congestion was found within 12 to 24 h (Figure 4). The liver and spleen showed dark reddish discoloration, which started to appear at 8 h. These changes were presented in the lower portion of the abdominal quadrants due to hypostatic congestion, as shown in Figure 5. Lividity increased in size and spread all over the dependent regions, and intensified at around 12 to 24 h. The lividity of each animal varied from red to purple and became darkened as the postmortem interval increased.

Decomposition or disintegration of the internal organs also occurred at different rates. The pancreas, gastrointestinal tract, livers, and thyroid showed marked autolysis early in PMI. At 8 to 12 h postmortem, the pancreas and its surrounding fat were soft and reddish, and appearances were similar in all animals (Figure 6A, B). Stomach and gastric mucosa began to soften and lost mucosal folds or rugae. The intestinal lumen was filled with gas, especially in the cecum, and distention and displacement of abdominal organs were found, as shown in Figures 8A, B. The results suggest that bacteria fermentation and gas formation could cause the organ to change position. The thyroid glands were pink to red in color. Moreover, the surface tissue collapsed, softened, and became flabby. Finally, the observation of the livers during these hours showed that the organs became darkened, shrinken, and spongy.

After 24 - 48 hours of PMI, severe autolysis and dissolution of most abdominal organs could be seen at this stage. The pancreas became more softened and liquefied, with tissue breakdown observed (Figure 6C). The results from 48 h postmortem revealed a thin gastric wall and reddish external surface in the stomach portion, which contacted the liver. The gastric mucosa was soft, liquid-like, and there were no rugae in the glandular stomach (Figure 7). The serosal surface of small intestine, large intestine, and mesenteries showed reddish coloration and a thin intestinal wall. A torsion or twist was also found at random parts of the intestinal tract (especially the part of jejunum and ileum) in 3 animals of the 48 h group, as shown in Figure 8D. Some areas of the livers were found to be pale. Another important aspect of this stage was the collapse and softness of many organs. 24 h postmortem, the internal organs including thyroid, livers, spleen, and kidneys were soft, flabby, and congested, as observed macroscopically (Figure 9). Then, 48 h postmortem, the organs of all animals showed an increasing degree of softening and more collapse; the kidneys presented a loss of normal architecture (Figure 10). Moreover, the liquefaction of abdominal fat was also present.

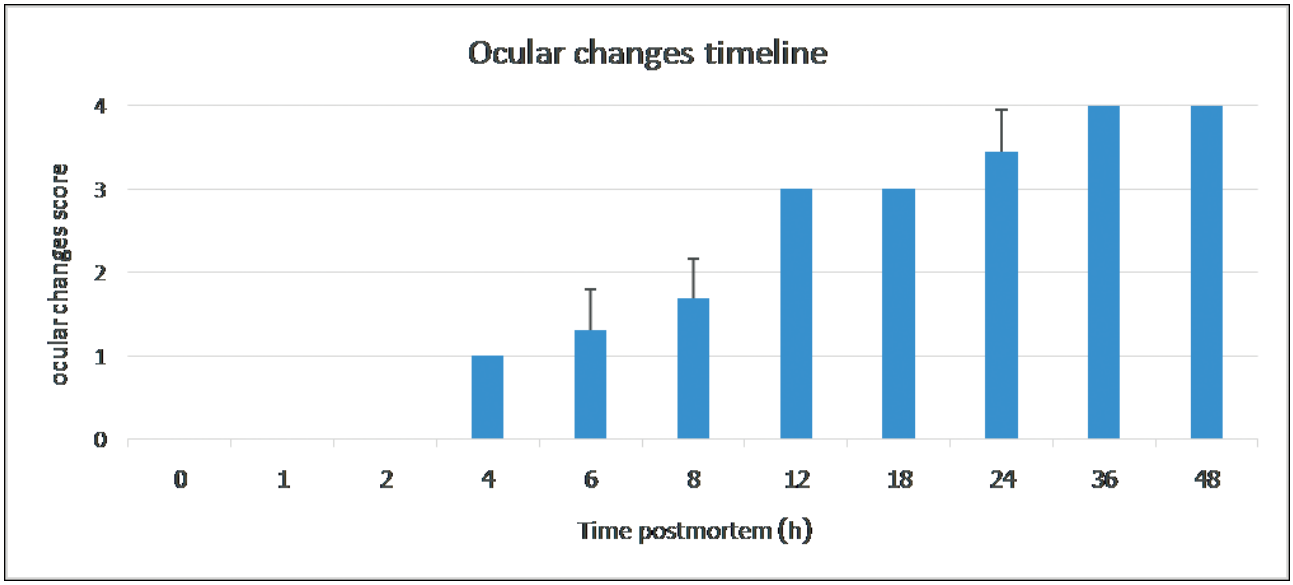

Figure 1. Timeline of postmortem ocular changes in rats (Mean ± SD, n=16).

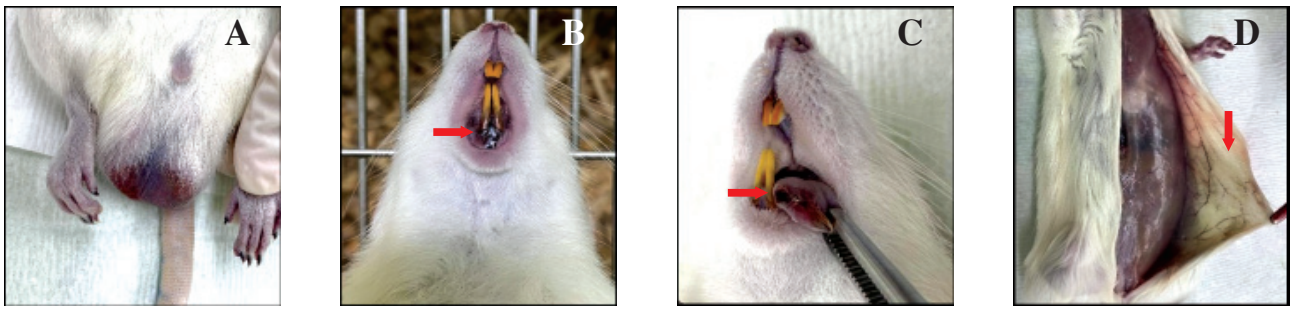

Figure 2. Discoloration of A) the skin on the scrotum and nails shown as dark red, B) gums shown as dark red, C) the tip of the tongue revealed as dark red in appearance, and D) abdominal skin shown as green discoloration.

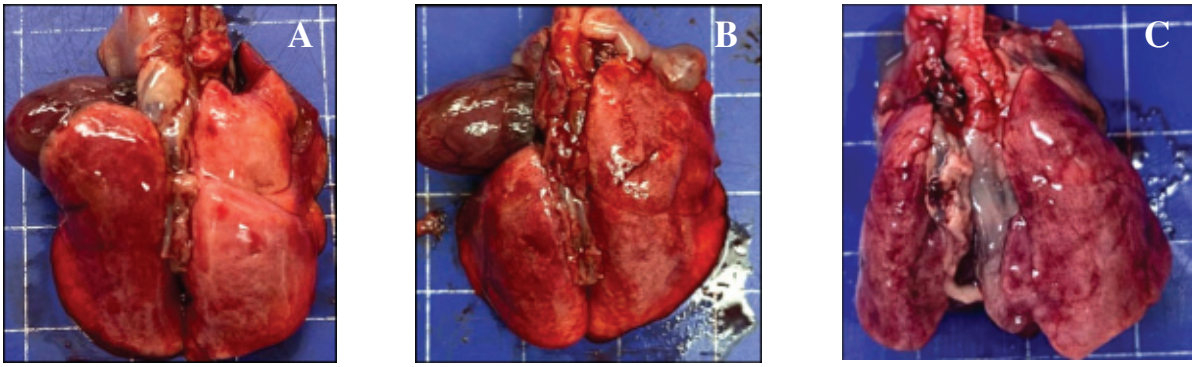

Figure 3. Livor mortis of the lung at A) 4 h PMI, with lungs exhibiting a dark purple area and congestion, B) 12 h PMI, exhibiting diffuse congestion in all lobes, and C) 48 h PMI, showing severe congestion and shrinkage.

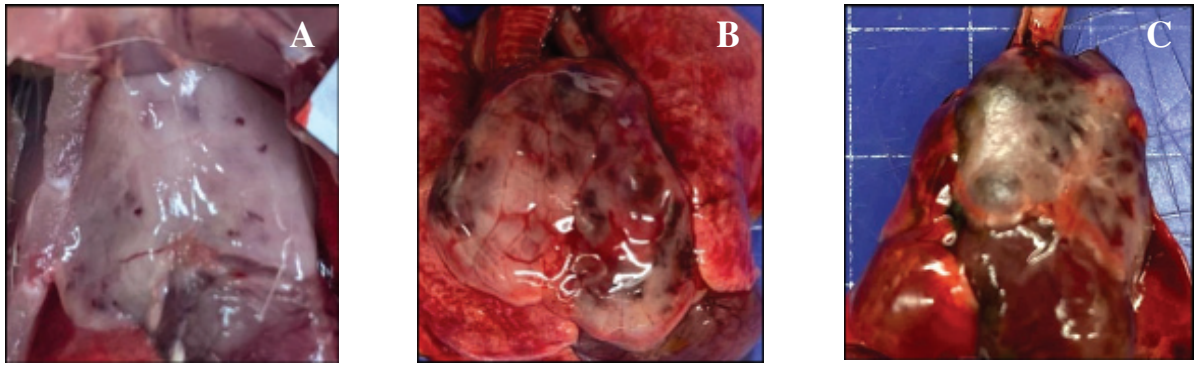

Figure 4. Livor mortis of the thymus at A) 8 h PMI, revealing reddish-purple spots, B) 12 h PMI, showing severe congestion, and C) 24 h PMI, also showing severe congestion.

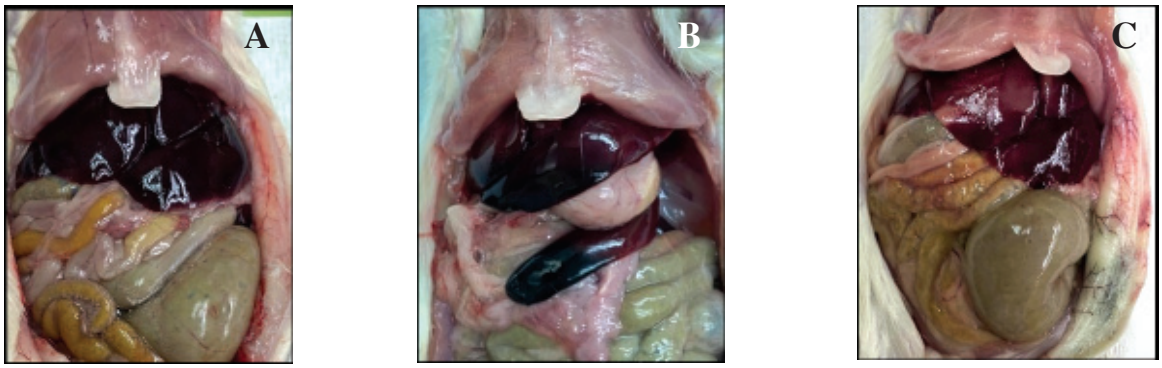

Figure 5. Livor mortis of the liver and spleen at A) 4 h PMI, with no apparent changes were found, B) 8 h PMI, with the liver and spleen showing reddish-blue staining of the low-lying dependent regions of the body, and C) 24 h PMI, revealing an increase in the extent of lividity.

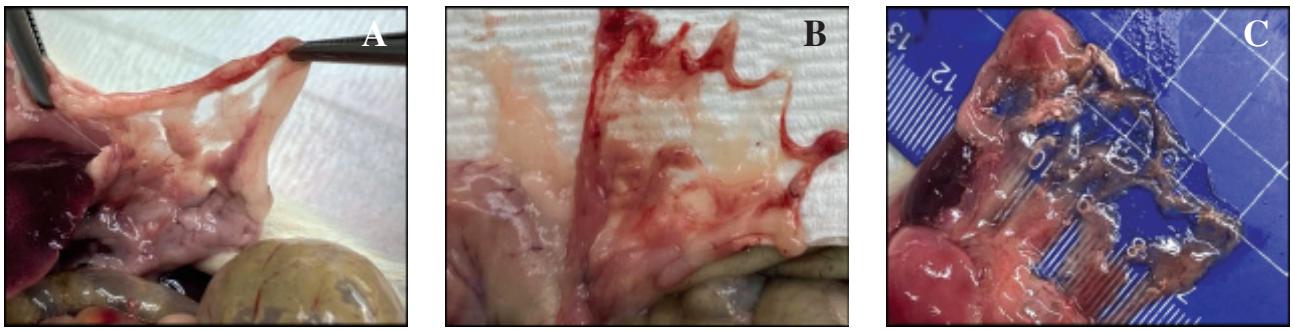

Figure 6. Decomposition changes in the pancreas at A) 4 h PMI, showing soft tissue. B) 12 h PMI, showing soft, and red coloration, and C) 48 h PMI, revealing an increased level of softening, almost liquefied, and breakdown of tissue.

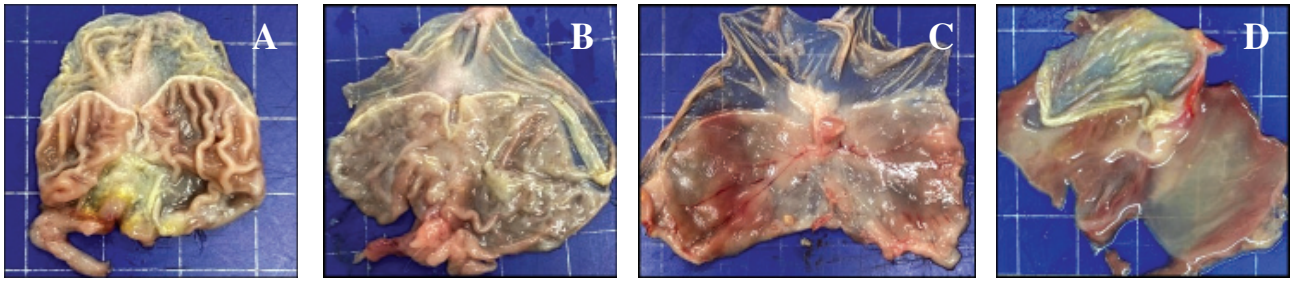

Figure 7. Gastric mucosal surface at A) 4 h PMI, with no apparent changes found, B) 12 h PMI, which found gastric mucosa beginning to soften and less mucosal folds or rugae, C) 24 h PMI, which revealed a thin gastric wall and a red stain on the external surface, while gastric mucosa was soft and rugae was lost, and D) 48 h PMI, were almost liquid.

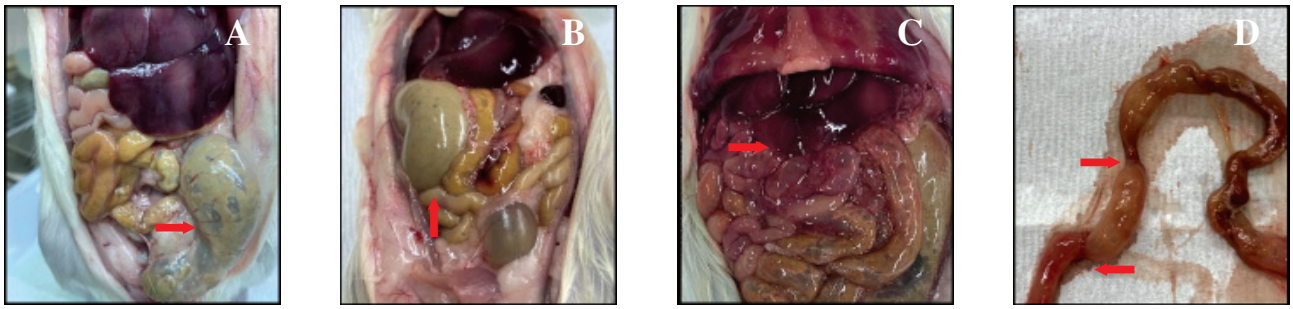

Figure 8. A, B) Intestinal distension and displacement causing changes in the position of organs (8 to 12 h PMI). C) Pinkish- red stain stain on the serosal surface of intestines and thin intestinal wall observed (12 to 48 h PMI). D) Intestinal torsion (48 h PMI).

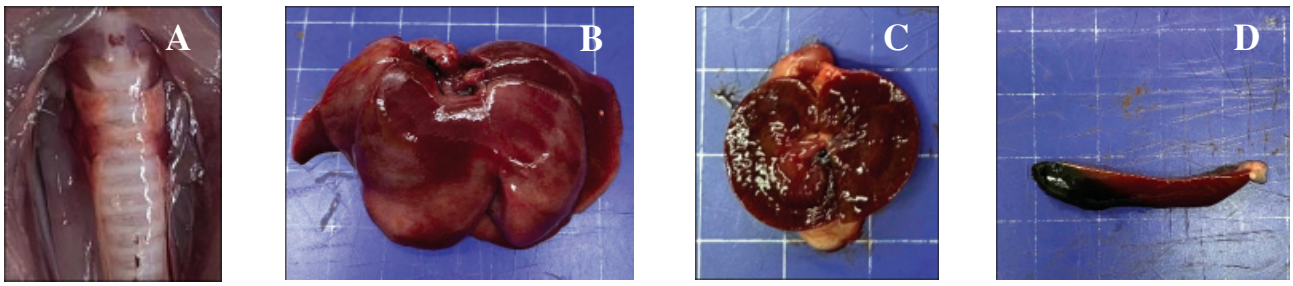

Figure 9. Decomposition changed in 24 h PMI. A) Thyroid were soft, collapsed and congested. B) Livers were soft and congested. C) Kidneys were soft. D) The spleen presented as congested and flabby.

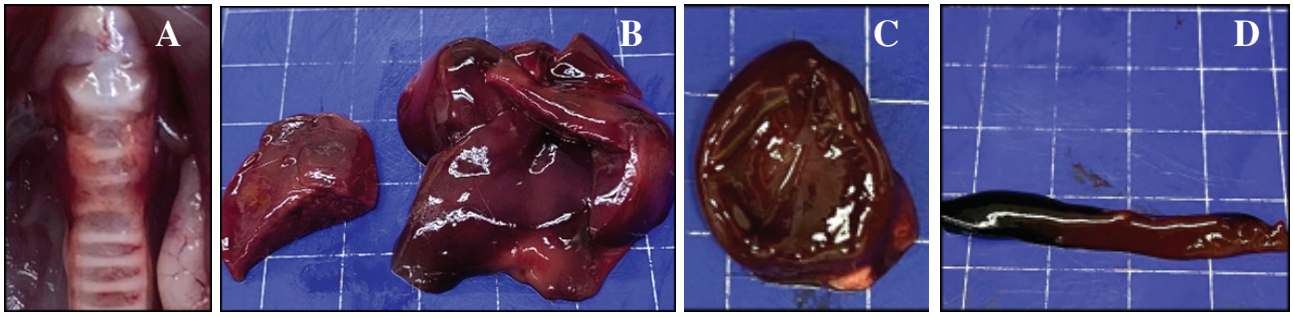

Figure 10. Decomposition changed in 48 h PMI. A) Thyroid presented as more collapsed, soft and flabby. B) Livers were soft, congested, and collapsed. C) Kidney were also soft, flabby and had lost of normal architecture (the cortex and medulla of the kidneys were difficult to distinguish). D) The spleen presented as soft, flabby, and congested.

Discussion

The study focused on the macroscopic changes in laboratory rat carcasses. The experiment was designed to prove the basic concepts of gross findings and related timelines of PMI in rats under laboratory animal house conditions. Interestingly, various changes in rat carcass were found at different times.

In the first examination, ocular changes during the early postmortem period included corneal opacity and sunken eyes. The results found that ocular changes in rat began with clouding at 4 h and evolved to complete total opacity after 6 h postmortem. The total sinking of the eyeballs occurred about 24 h postmortem. The results from this study are similar to data published by Capas-Peneda et al. (2016), in which rats showed total corneal opacification presented at 5 h postmortem, and total eye sinking was evidenced for nearly 20 h. In mice, corneal opacification was completed within the first-hour postmortem, and total eye sinking occurred approximately 19 h postmortem (Capas-Peneda et al., 2016). The results of eye changes are difficult to compare with other animal and human because it depends on whether the eyelids are open or closed. Many studies have also found that pattern changes in the eyes are associated with PMI, such as corneal opacity, pupillary diameter, retinal vessel striation, retinal color changes, and intraocular pressure (Kumar et al., 2012; Salam et al., 2012). Among these patterns, intraocular pressure and corneal opacity were the most significantly related to PMI (Balci et al., 2010; Brook 2016).

The earliest postmortem changes occurred while the body was still in the fresh stage before the breakdown of soft tissues, including rigor mortis and livor mortis. These are of forensic significance (Poloz and O'Day 2009).

Livor mortis (lividity or postmortem hypostasis) is the settling of blood to the downside of an animal body and the gravitational settling of blood and body fluids. This phenomenon results in darker reddish coloration on the downside of the carcass. In this study, livor mortis was apparent as discoloration presented in the mucous membranes (lips, gums, around the eyes) and nails. At the early stages of livor development, the color was red due to the oxygenation of red blood cells. It became darker over time as oxygen levels declined or oxygen dissociation continued after death, resulting in a darker or reddish-purple color (Pounder 2011). Livor mortis could also be found on the internal body surfaces and internal organ, most noticeably on the surface of the lungs. Vascular congestion of the lungs is considered one of lividities. The congestion of blood vessels in the lung is derived from an excess of normal blood and fluid settling or hypostasis which occurs spontaneously in the postmortem period (Perper 2006).

This study found that lividity could be detected as early as 4 - 8 h and was found in the lung, thymus, liver, and spleen. Subsequently, it intensified at around 12 to 24 hours. These results make it difficult to compare times with other rodents or animals because studies on animals comprise limited information. In a human study, livor mortis can be found at several positions, such as externally in the skin and mucous membranes and internally in the abdominal or thoracic viscera. It typically developed within 30 minutes to 2 h (Di Maio and Di Maio 2001) and is fully developed at approximately 10 to 12 h after death (Lew 2005). However, lividity of the internal organs could be misinterpreted as congestion or injury (Perper 2006). In humans, the rate of livor mortis was found to either increasing with accelerated decomposition or decrease with cool ambient temperatures,

constant by 24 to 36 h (DiMaio and DiMaio 2001). However, the appearance of livor differs markedly from case to case due to the environment, location, species, body size, discoloration pattern, and the events surrounding death.

Two mechanisms of autolysis and putrefaction are involved in the process of decomposition. Although decomposition occurs immediately after death through autolysis, macroscopic changes only become notable later when putrefaction has occurred (Cockle and Bell 2017). Autolysis is tissue softening and liquefaction caused by the release of intracellular enzymes, resulting in the breakdown of tissue and organs. Organs containing higher enzymes, such as the pancreas and liver, are autolyzed more rapidly (Merck 2013). From the dissection data in this study, the pancreas was the first tissue that appeared to show autolysis. Next, the changing of the liver was seen. These appearance could be found early in 8-12 PMI.

Putrefaction is the decomposition of the body by the action of microorganisms. After cessation of homeostasis, the body's normal flora migrates from the intestinal lumens to the blood vessels and spreads throughout the body (Elliott et al., 2004). The earliest decomposition change occurs because of the degradation of hemoglobin and the formation of hydrogen sulfide (H_2S) within vessels and tissues by the anaerobic process of bacteria. The reaction of both compounds produced green coloration in the lower abdomen (Amendt et al., 2004). In addition, this study observed the greenish discoloration of the skin over the abdomen, which was the first external sign of putrefaction due to the process previously described above.

In our results, the dark green/purple discoloration of the abdomens of rats was found within 12 h postmortem. In a dog study, greenish discoloration could be found 24 h postmortem (Erlandsson and Munro 2007). The quantity of gas was directly proportional to the increasing bacterial activity. Hydrogen sulfide causing the distension of the abdomen and purging putrefactive liquids from the mouth and nostrils was reported in human autopsy (Lee Goff 2009). Bloating is caused by putrefactive gases, H_2S, being trapped within the body. These gases cause distension of the abdominal organs. As a result, displacement will be found in the abdominal organs (Simmons and Cross 2013). This study found intestinal displacement within 8 to 12 h PMI and torsion of the intestines, even breaking part of the tract at 48 h postmortem. The liver also revealed paleness in different areas due to the pressure exerted by the distended gastrointestinal tract. The time found in this study is probably different from humans and other animals. One study showed that distention is typically most notable in the abdomen and often develops at approximately 60 to 72 h in humans. Meanwhile, abdominal distention may occur with remarkable rapidity in ruminants, this process may occur significantly faster or slower depending on the environmental conditions (Munro and Munro 2008).

Morphological changes were observed in the gastrointestinal tract, from necropsy at 12 h. The results showed pinkish to reddish stains on the outer surfaces of stomach, intestine, and surrounding fat. This is known as hemoglobin imbibition, which is caused by the lysis of red blood cells after autolysis and putrefaction. Moreover, all organs found putrefaction started to appear within 8 to 12 h after death and fully developed within 24 to 48 h. The main changes found included discoloration, softening, and liquefaction. Different from human data,

putrefaction began within an hour of death and the highest microbial activity occurred within the 24 h (Shedge et al., 2021). The fermentation process caused softening and liquefaction of the soft tissues by transforming carbohydrates, lipids, and proteins into organic acids and gases (Byard and Tsokos 2013).

The general physical changes, decomposition stages, autolytic activity, and structural alterations in tissue were primarily detected by observation. Postmortem period characteristic changes include livor mortis, discoloration, ocular change, and gross change. These parameters are helpful for the estimation of the time since death or PMI. However, it highly depends on individuals and environmental factors such as temperature, humidity, cause of death, age, body size, initial pathological conditions, etc. (Henssge and Madea 2007).

In conclusion, it is possible to apply different characteristics from general appearances and necropsy data to refine the estimation of the PMI in rats, based on ocular change and gross observation. In this study, the ocular changes, macroscopic changes in the lung, thymus, liver, spleen and the decomposition of abdominal organs proved to be the most useful organs, highlighting the changes that developed during the 48 h timeframe after death. These data could aid in indicating postmortem and antemortem to prevent misinterpretation. Moreover, PMI could be estimated by evaluating the morphological findings. Analysis of PMI degradation is a primary tool for death investigation in the laboratory rats, which benefits researches and veterinarians. Future research is expected to result in better techniques with increased accuracy in PMI estimation and postmortem change studies in several laboratory animals, which will further beneficial veterinary forensic investigations.

Acknowledgements

The authors would like to acknowledge the help and support from the all the staffs from National Laboratory Animal Center at Mahidol University.

References

Amendt J, Krettek R, Zehner R. Forensic entomology. Naturwissenschaften. 2004;91(2):51-65.

Balci Y, Basmak H, Kocaturk BK, Sahin A, Ozdamar K. The importance of measuring intraocular pressure using a tonometer in order to estimate the postmortem interval. Am J Forensic Med Pathol. 2010;31(2):151-5.

Brooks JW. Postmortem Changes in Animal Carcasses and Estimation of the Postmortem Interval. Vet Pathol. 2016;53(5):929-40.

Byard RW, Tsokos M. The challenges presented by decomposition. Forensic Sci Med Pathol. 2013;9(2): 135-7.

Capas-Peneda S, Gonçalves-Monteiro S, Oliveira B and Duarte-Araùjo M. How do you tell how long has a mouse been dead? Rigor mortis as a tool to estimate mice time of death (TOD) in animal house facilities. 13th FELASA Congress 2016.

Cockle DL, Bell LS. The environmental variables that impact human decomposition in terrestrially exposed contexts within Canada. Sci Justice. 2017;57(2):107-17.

DiMaio VJ, DiMaio D. Forensic Pathology. New York: CRC Press; 2001.

Elliott S, Lowe P, Symonds A. The possible influence of micro-organisms and putrefaction in the production of GHB in post-mortem biological fluid. Forensic Sci Int. 2004;139(2-3):183-90.

Erlandsson M and Munro R. Estimation of the post-mortem interval in beagle dogs. Sci Justice. 2007;47:150-4.

Henssge C, Madea B. Estimation of the time since death. Forensic Sci Int. 2007;165(2-3):182-4.

Krompecher T. Rigor mortis: Estimation of the time since death by evaluation of cadaveric rigidity. In: Madea B, editor. Estimation of the time since death. 3rd ed. London: CRC Press; 2016. p. 41-58.

Kumar B, Kumari V, Mahto T, Sharma A, Kumar A. Determination of Time Elapsed Since Death from the Status of Transparency of Cornea in Ranchi in Different Weathers. J Indian Acad Forensic Med. 2012;34(4):336-8.

Lee Goff M. Early post-mortem changes and stages of decomposition in exposed cadavers. Exp Appl Acarol. 2009;49(1-2):21-36.

Lew E, Matshes E. Postmortem changes. In: Dolinak D, Matshes E, Lew E, editors. Forensic Pathology: Principles and Practice. NewYork: Elsevier/ Academic Press; 2005. p. 527-54.

Lowe AC, Beresford DV, Carter DO, Gaspari F, O'Brien RC, Stuart BH, et al. The effect of soil texture on the degradation of textiles associated with buried bodies. Forensic Sci Int. 2013;231(1-3):331-9.

Megyesi MS, Nawrocki SP, Haskell NH. Using accumulated degree-days to estimate the postmortem interval from decomposed human remains. J Forensic Sci. 2005;50(3):618-26.

Merck M, Miller DM. Postmortem changes and the postmortem interval. In: Merck M, editor. Veterinary Forensics: Animal Cruelty Investigations 2nd ed. Ames, IA: John Wiley; 2013. p. 255-71.

Munro R, Munro HM. Animal abuse and Unlawful killing: forensic veterinary pathology. Philadelphia: Saunders/Elsevier. 2008.

Munro R, Munro HM. Some challenges in forensic veterinary pathology: a review. J Comp Pathol. 2013;149(1):57-73.

Perper JA. Time of death and changes after death, Part 1: Anatomical considerations. In: Spitz WU, Spitz DJ, editors. Medicolegal investigation of death. Guidelines for the application of pathology to crime investigation, 4th ed, Springfield: Charles C. Thomas Publisher, Ltd; 2006. p. 87-127.

Poloz YO, O'Day DH. Determining time of death: temperature-dependent postmortem changes in calcineurin A, MARCKS, CaMKII, and protein phosphatase 2A in mouse. Int J Legal Med. 2009;123(4):305-14.

Pounder D. Time of Death. Lecture notes for Forensic Medicine Course, Department of Forensic Medicine, University of Dundee, Dundee, Scotland. 2011.

Salam HA, Shaat EA, Aziz MM, MoneimSheta AA, Hussein H. Estimation of postmortem interval using thanatochemistry and postmortem changes. Alexandria J. Med. 2012;48:335-44.

Shedge R, Krishan K, Warrier V, Kanchan T. Postmortem Changes. StatPearls. Treasure Island (FL): StatPearls Publishing Copyright? 2021, StatPearls Publishing LLC.; 2021.

Simmons T, Cross PA. Forensic Taphonomy. In: Siegel JA, Saukko PJ, Houck MM, editors. Encyclopedia of Forensic Sciences. 2nd ed. Waltham: Academic Press; 2013:12-7.

Sutherland A, Myburgh J, Steyn M, Becker PJ. The effect of body size on the rate of decomposition in a temperate region of South Africa. Forensic Sci Int. 2013;231(1-3):257-62.

Syabani DM, Eliyani H, Suharsono S, Rantam FA, Ma'ruf A. Postmortem Interval Estimation Time from Algormortis Temperature of Rats Expressed by MARS Model Approach. KnE Life Sci. 2017: 3(6): 404-12.

Case Report

Feline Portosystemic Shunts: A Case Report

Poonnut Darakamas[1*] Panyakamol Chandrasakha[1] Sukanya Maneein[2]
Rungrote Osathanon[2] Pasakorn Brikshavana[3] Krittin Chuaychoo[1]
Namphung Seumanotham[2]

[1]Prasuarthon Animal Hospital, Faculty of Veterinary Sciences, Mahidol University,
Phuttamonthon 4 Rd., Salaya, Nakhon Pathom 73170, Thailand
[2]Department of Veterinary Clinical Sciences and Public Health, Faculty of Veterinary sciences, Mahidol University,
Phuttamonthon 4 Rd., Salaya, Nakhon Pathom 73170, Thailand
[3]Kaewkarn Animal Hospital,
Bang Na-Trat Road., Bangkaew sub-district, Bangphe district Samutprakarn 10540, Thailand

[*]Corresponding author, E-mail address: poonnut.dar@mahidol.edu

Received: 27 June 2022; Revised: 23 August 2022; Accepted: 24 August 2022

Abstract

A 4 kg, 3 year-old, spayed female, Persian cat was presented at Prasuarthon Animal Hospital, Faculty of Veterinary Science, Mahidol University with the clinical sign of ptyalism for the past year. Two days before the visit, the owner reported a behavioral change, circling and obtunded. From the physical examination, all vital signs were normal. Hematological values were within reference interval. However, serum ammonia and pre-prandial post-prandial bile acid were elevated. Thoracic radiographic and abdominal ultrasonographic findings were unremarkable. Computed tomography (CT) result revealed the left gastro-caval shunt with portal hypertension. The cat was diagnosed as feline extrahepatic portosystemic shunt. Surgical excision was applied with cellophane banding. The cat was admitted for post-operative care for 7 days. During the hospitalization, pain assessment was monitored with systolic blood pressure and closely observed the clinical sign of seizure. Moreover, abdominal ultrasonography was performed to monitor ascites and peritonitis. The ammonia and pre-prandial/post-prandial bile acid tests were done on day 1, 7 and 120 after surgery which displayed within normal range. The cat did not express ptyalisim or neurological disorders such as seizure after surgery during the observation period more than 120 days. This case report aimed to describe a successful treatment of portosystemic shunt in a cat.

Keywords: Portosystemic shunts, PSS, Ammonia, Cellophane banding

รายงานสัตว์ป่วย: โรคเส้นเลือดลัดข้ามตับในแมว

ปุณณัตถ์ ดาระกะมาศ[1*] ปัญญกมล จันทรสาขา[1] สุกัญญา มณีอินทร์[2] รุ่งโรจน์ โอสถานนท์[2]
ภาสกร พฤกษะวัน[3] กฤติน ช่วยชู[1] น้ำผึ้ง สื่อมโนธรรม[2]

[1]โรงพยาบาลสัตว์ ประศุอาทร คณะสัตวแพทยศาสตร์ มหาวิทยาลัยมหิดล
ถนนพุทธมณฑลสาย 4 ตำบลศาลายา อำเภอพุทธมณฑล จังหวัดนครปฐม 73170
[2]ภาควิชาเวชศาสตร์คลินิกและการสาธารณสุข คณะสัตวแพทยศาสตร์ มหาวิทยาลัยมหิดล
ถนนพุทธมณฑลสาย 4 ตำบลศาลายา อำเภอพุทธมณฑล จังหวัดนครปฐม 73170
[3]โรงพยาบาลสัตว์แก้วกาญจน์
ถนนบางนา-ตราด ตำบล บางแก้ว อำเภอ บางพลี จังหวัด สมุทรปราการ 10540

[*]ผู้รับผิดชอบบทความ E-mail address: poonnut.dar@mahidol.edu

Received: 27 June 2022; Revised: 23 August 2022; Accepted: 24 August 2022

บทคัดย่อ

แมวตัวเมีย พันธุ์เปอร์เซีย อายุ 3 ปี น้ำหนัก 4 กิโลกรัม มาพบด้วยปัญหา น้ำลายไหลมากมาเป็นเวลามากกว่าหนึ่งปี และยังพบอาการเดินวน พฤติกรรมเปลี่ยน ตรวจร่างกายลักษณะภายนอกโดยรวมปกติและ ตรวจเลือดเพิ่มเติม พบค่าเลือดโดยรวมปกติ แต่พบค่าแอมโมเนีย ค่าการทำงานถุงน้ำดี มีค่าสูงขึ้นกว่าปกติ หลังจากนั้นจึงได้ทำการการตรวจวินิจฉัยทางรังสีวินิจฉัย ผลการตรวจวินิจฉัย พบว่าแมวป่วยเป็นโรคเส้นเลือดลัดข้ามตับ (Portosystemic shunts) แมวได้รับการรักษาโดยการผ่าตัดโดยใช้เทคนิค cellophane banding หลังจากผ่าตัดแมวพักฟื้นที่โรงพยาบาลสัตว์ประศุอาทร เป็นเวลา 7 วัน มีการควบคุมความเจ็บปวดและติดตามอาการอย่างใกล้ชิด การศึกษาดังกล่าวได้ติดตามอาการของสัตว์ป่วยทั้งสิ้น 120 วัน ได้มีการตรวจระดับแอมโมเนียและค่าการทำงานของถุงน้ำดี ในวันที่ 1, 7 และ 120 ของการศึกษาติดตามอาการ โดยพบค่ากลับมาปกติ นอกจากนั้น แมวไม่แสดงอาการเดินวน อาการทางระบบประสาทอื่นๆ น้ำลายไหลมากกว่าปกติอีกเลย การติดตามทั้งสิ้นใช้เวลาถึง 120 วัน และกรณีศึกษาดังกล่าวนับเป็นความสำเร็จของการผ่าตัดและรักษาแมวเพื่อให้คุณภาพชีวิตแมวดีขึ้นได้นั่นเอง

คำสำคัญ : Portosystemic shunts เส้นเลือดข้ามตับ แอมโมเนีย Cellophane banding

Introduction

Feline portosystemic shunts (PSS) are uncommon vascular abnormalities that cause blood to bypass the liver (Devriendt et al., 2020), resulting in neurological symptoms such as seizures and ptyalism, as well as gastrointestinal and urinary tract signs (Tivers and Lipscomb 2011a). Normally blood drains the stomach and the intestine enters the portal vein, travels through the liver via the hepatic vein, and then to the caudal vena cava but PSS blood from portal vein will bypassing from hepatic (Berent and Tobias 2009). The hepatic function about urea synthesis is also known as the Krebs-Henseleit cycle from intramitochondrial production that change ammonia to urea (Dimski 1994). There are two major types of portosystemic shunts, congenital and acquired. Congenital PSS is commonly seen in small or toy breeds dogs and cats (Hunt et al., 2004b). Young cats may have congenital shunts which can be categorized into extrahepatic and intrahepatic shunts, while acquired PSS usually caused extraheptatic shunt. (Papamichail et al., 2018). An intrahepatic shunt is a vessel that connects the liver to the body (Blaxter et al., 1988). The common breeds with extrahepatic shunt are domestic shorthairs, Persian, British shorthair, Ragdoll, domestic longhair, Birman, British blue and Tonkinese (Lipscomb et al., 2007; Tivers and Lipscomb 2011b). Extrahepatic shunt most frequently located near the kidney caused by hepatic cirrhosis, non-cirrhotic portal hypertension such as hepatic arteriovenous malformation, and hepatic portal venous hypoplasia (Berent and Tobias 2009). In cats, a single extrahepatic vessel entering the caudal vena cava into left gastric vein is the most common form of a congenital portosystemic shunt (Blaxter et al., 1988) .

The type of shunt (intrahepatic or extrahepatic) must be confirmed by using ultrasonography, mesenteric portovenography, computed tomography (CT) or magnetic resonance imaging (MRI) (Tivers and Lipscomb 2011a). Blood examination should be monitored for ammonia, bile acid, coagulopathy, urinalysis, liver enzyme activities, and blood urea nitrogen (Tillson and Winkler 2002a).

Surgery is the treatment of choice for most cats with PSS and medical management is aimed to treat the clinical signs (Valiente et al., 2020). The methods for surgical correction by using extravascular techniques have been reported in cat including ameroid constrictor and cellophane band (Valiente et al., 2020). Ameroid constrictor and cellophane band can cause a tissue reaction in difference ways to slowly attenuate the portosystemic shunt by inducing luminal pressure from thrombosis of the shunt as well as a perivascular reaction which lead to fibrosis (Tobias 2009; Joffe et al., 2019). This procedure focuses on producing a complete shunt decrease causing portal hypertension (Valiente et al., 2020). Postoperative complications in cat after surgical attenuation are common signs of neurological disorders, including seizure (Ruland et al., 2009b). Hypertension and ascites can be found as a resulting of portal hypertension (Buob et al., 2011). This case report aimed to describe a successful for treatments of feline PSS

Case description

A 4 kg, 3 year-old, spayed female, Persian cat had been suffering from depression and ptyalism for the past year. Two days before coming to Prasuarthon Animal Hospital, Faculty of Veterinary Science, Mahidol University, the owner reported a behavioral change, circling and intense depression. This was the first time that the cat visited to animal hospital for illness. The cat was a fully vaccinated and lived indoor with other 11 cats.

On the physical examination of the cat from the first visit, the body condition score was 3/9 and oral cavity was normal with pink mucous membrane. Heart rate, heart sound, respiratory rate and lung sound were normal. Intermittent neurological signs showed dilation of pupils and ataxia. Head shaking, tongue protrusion and muscle tremor were also presented.

Complete blood count (CBC), biochemistry included creatinine, blood urea nitrogen (BUN), liver enzyme, coagulation profile, urinalysis and all other laboratory values were within normal limits (Table 1) excepted serum ammonia and prepradial-postpradial bile acid. Blood ammonia and bile acid concentration was higher than referent range (Table 2), Suspected problem of hepatic function including portosystemic shunt is one of differential diagnosis.

Abdominal radiography showed normal organs in normal position from both ventrodorsal and lateral views. Liver and spleen were unremarkable. Urinary bladder was normal without radiopaque urolith, and normal vertebrae without spondylosis from this radiography (Figure 1). Abdominal ultrasonography revealed that the liver was slightly small with hyperechoic parenchyma, the portal vein and mesenteric vein were dilated and slightly torturous, no any extra hepatic shunts were found. Both kidneys had hyperechoic renal cortex with decreased corticomedullary junction (CMJ) differentiation and mild irregular shape (Figure 2). Abdominal radiography and ultrasonography were unable to rule in PSS. The cat was then generally anesthetized for CT scan of the abdomen with intravenous contrast. The result showed a small size liver with irregular margin. The portal vein was small, a large tortuous shunt vessel arises from the portal vein, courses caudally, to the left cranially past the diaphragm then turning rightward to terminate on the caudal vena cava (CVC), the diameter of this vessel was around 8 mm where it began, the left gastro-caval shunt was suspected with portal hypertension, chronic hepatopathy, splenomegaly (Figure 3). In conclusion, the cat was diagnosed as feline extrahepatic portosystemic shunt.

One month prior to the surgery, the cat was fed with a commercial hepatic diet (Royal canin®, Aimargues, France), for the purpose of reducing blood urea. The cat received 2 milliliter lactulose (Hepalac®, Osoth inter Laboratories CO., LTD., Thailand) two to three times a day to decrease ammonia production approximately one week prior. Hepatic supportive was by milk thistle (Samarin®, Berlin Pharmaceutical Industry CO., LTD., Thailand), and treated with metronidazole 10 mg/kg (Metrolex®, Siam Pharmaceutical Co., Ltd., Thailand). The primary goal is to control anaerobe bacteria population in the intestine and prevent reinfection.

For the surgical procedures, cellophane technique was applied. The advantage for using cellophane is the incident of a life-threatening portal hypertension was very low, however, wider bands or failure to promote shunt closure can develop a multiple acquired shunts. Started with acepromazine 0.04 mg/kg (Combistress®, Kela N.V., Belgium) was used as a premedication, combined with morphine 0.3 mg/kg (M&H Manufacturing Co., LTD, Thailand) intramuscularly administered for analgesia. Anesthetic induction was performed with intravenous alfaxalone 1 mg/kg (Alfaxan®, Accord Intertrade Co., Ltd., Bangkok, Thailand). The patient was endotracheal intubated and maintained the anesthesia with sevoflurance (Baxter Healthcare of Puerto Rico, USA) cefazolin 25 mg/kg (Cafaben®, L.B.S. laboratory LTD., PART., Thailand) and metronidazole 10 mg/kg (Metrolex®, Siam Pharmaceutical Co., Ltd., Thailand) were used as antimicrobial drugs. Inflammation and pain were controlled

by meloxicam 0.2 mg/kg (Metacam®, Labiana Life Sxience, S.A., Barcelona, Spain). The patient was undergone a ventral midline laparotomy. The liver lobes had yellow discoloration. Ventral leaf of the omentum was perforated and the shunt was found on the left side of the caudal vena cava, caudal to the stomach. Turbulent flow was observed within the shunt and 3-folded cellophane band with diameter of 3 mm was placed around the shunt and 4 surgiclips were placed to secure the cellophane. The diameter of shunts was approximately 7.6 mm. and the cellophane can provide the attenuation of the shunt to less than 3 mm. All vital signs including non-invasive measurement of systolic blood pressure were closely monitored. No signs of hepatic congestion and systemic hypertension were observed after placing the cellophane.

After surgery, the cat was hospitalized for 7 days. Pain assessment was counteracted with fentanyl in a constant rate infusion (CRI) monitored by using systolic blood pressure (Table 3). The cat showed no sign of seizure, which can cause by portal hypertension and any relating neurological symptoms such as acute blindness. Daily body weight (Table 3) was measured for monitoring the extravascular fluid leakage and accumulation such as ascites. Moreover, the abdominal ultrasonography was performed during the postoperative period to monitor the correction site of the previous shunt, ascites, peritonitis and hepatic morphology that showed no extrahepatic shunt. In addition, monitoring the location for surgiclips was also observed by using ultrasonography. Nonetheless, the procedure of using the cellophane band can provide a complete shunt closer around 60 ñ 90 days after surgery and the liver function test should be monitored, especially serum bile acid. This case was followed up for 120 days. Therefore, the ammonia test was performed on the first day post operation, 7 days and 120 days respectively (Table 2). Bile acid stimulation test was performed after 120 days (Table 2). After surgical correction, the level of serum ammonia and post bile acid was decrease gradually and was within normal reference range. This cat had no evidence of ptyalism, seizure, or neurological problems, and appeared to be a healthy cat. Hepatic diet was recommended to help in controlling the serum ammonia levels. Ideally, PSS patients should not require a long-term medical management. Lactulose was prescribed to titrate down and stopped for a minimum of 14-28 days, based on clinical signs and severity of the disease. After 48ñ56 days, normal diet may be considered or fed until animal expresses signs of improvement in hepatic function.

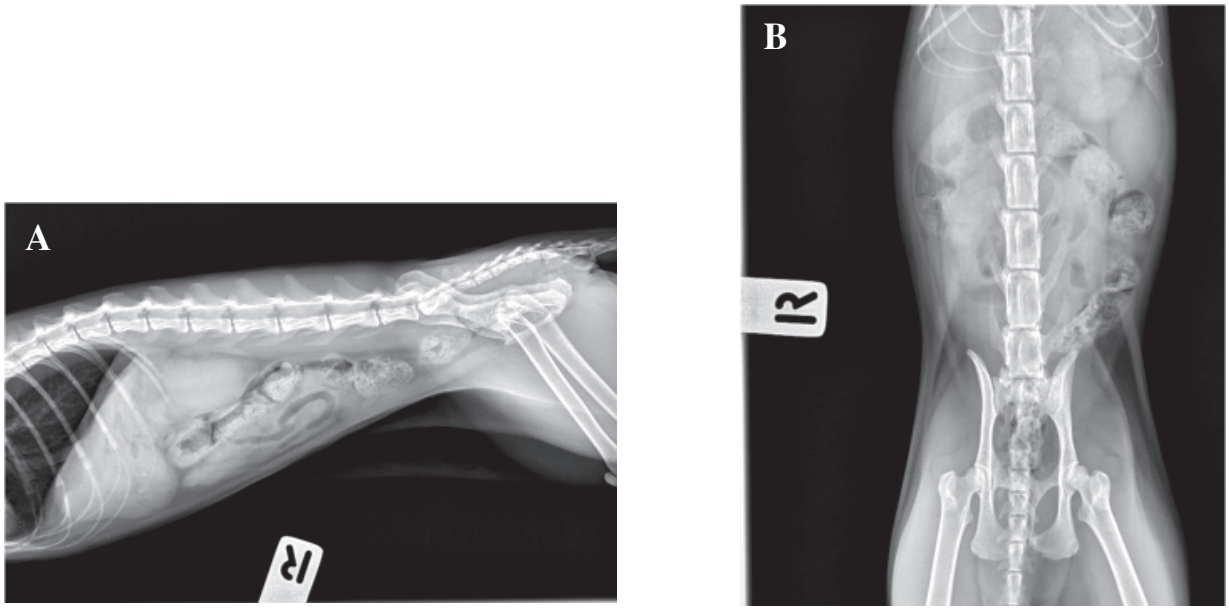

Figure 1. Lateral view (A) and ventro-dorsal (B) of plain abdominal radiograph revealed unremarkable lesion of abdominal organ.

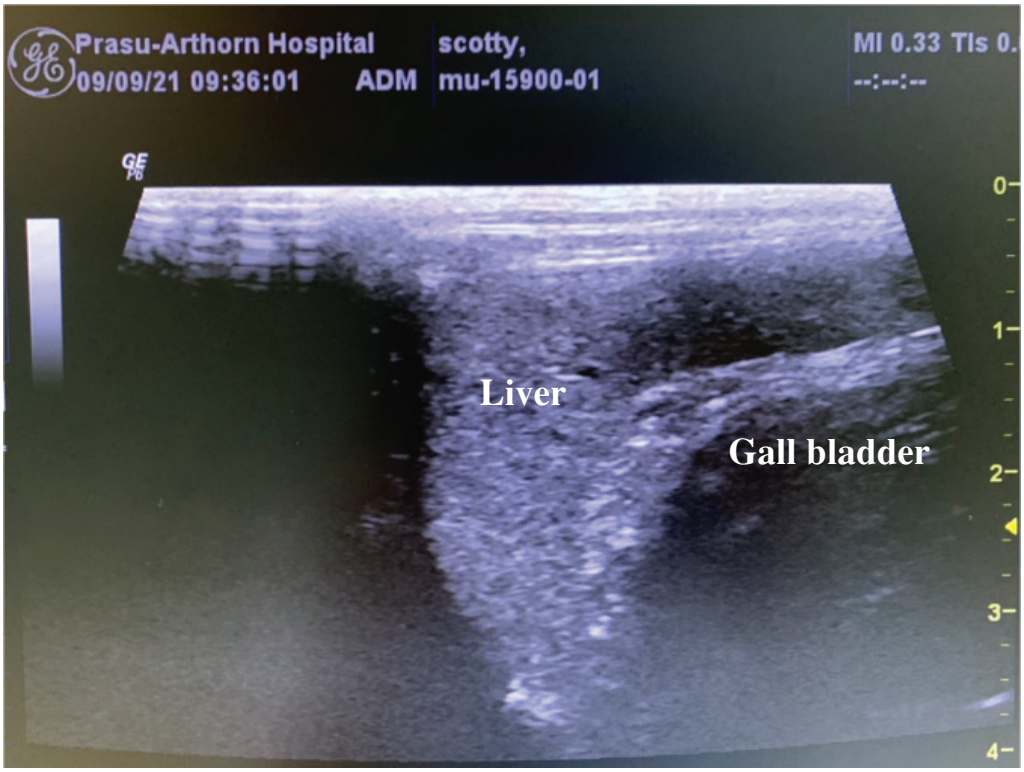

Figure 2. Ultrasonography showed unremarkable lesion of liver and gall bladder.

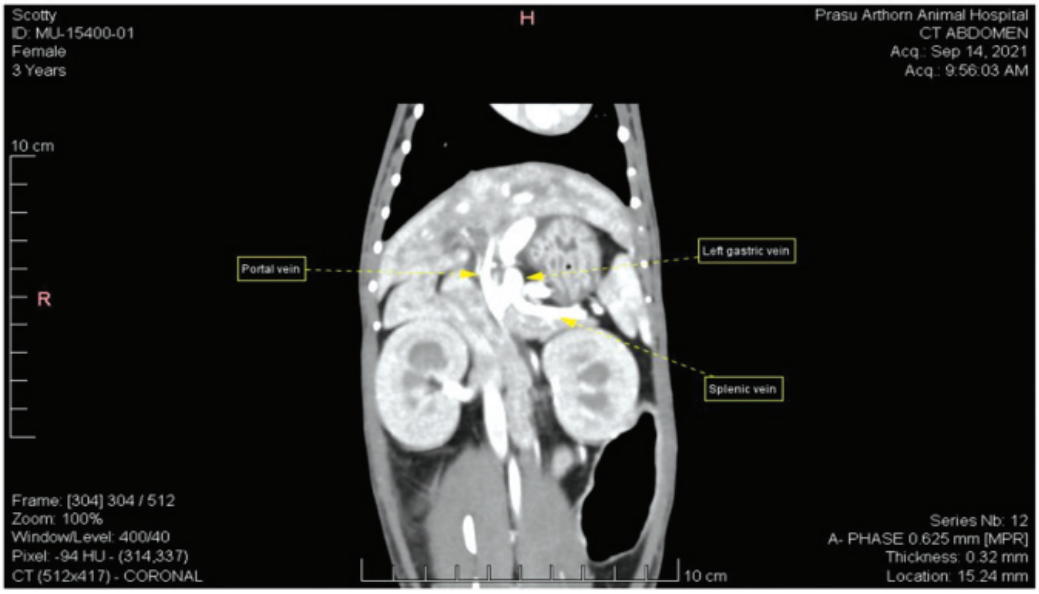

Figure 3. Left gastric vein reported from computed tomography (CT) angiography image of portosystemic shunt arising from the splenic vein.

Table 1. Hematological report and urinalysis from the first visit.

Parameters	Reference range	Day 0	Parameters	Reference range	Day 0
WBC (u/L)	5.5-19.0	10.44	Coagulation APTT	9.8-19.0	12.3
Monocyte	1-4	4	Coagulation PT	6.5-11.5	9.9
Neutrophil	35-75	72	Coagulation TT	15.1-25.7	18
Lymphocyte	20-55	24	SG	1.010-1.040	1.048
Eosinophil	2-12	0	pH		7.5
Basophil	0	0	LEU		2+
Hct (%)	5.0-10.0	29.2	NIT		-
RBC (106ul)	10-15.0	7.47	PRO		2+
Hb (g/dl)	30-45	10.3	GLU		2+
PLT (103/ul)	300-600	140	KET		-
BUN (mg/dL)	16-36	18	UBG		-
Creatinine (mg/dL)	0.8-2.4	1.14	BIL		-
ALT(U/L)	12-130	94	ERY		-
ALP (U/L)	14-111	50			

**Hct: hematocrit, PLT: platelet, RBC: red blood cell, Hb: hemoglobin, BUN: blood urea nitrogen, ALT: alanine aminotransferase, ALP: alkaline phosphatase, SG: specific gravity

Table 2. Serum ammonia and pre-prandial /post-prandial bile acid report after surgery.

Parameters	Reference range	Day 0	Day 1	Day 7	Day 120
NH3 (umol/L)	0-95	166	33	23	19
Preprandial (umol/L)	0-6.9	6.83	-	-	2.4
Postprandial (umol/L)	0-14	49.67	-	-	2.8

NH_3: ammonia

Table 3. Body weight and systolic blood pressure that show before surgery and postoperative.

Parameters	Day0	Day1	Day2	Day3	Day4	Day5	Day6	Day7
Body weight (kg)	4	4	4	4	4	4	4	4
Systolic blood pressure (mmHg)	170	150	130	130	120	120	120	120

Day 0: before surgery, Day 1-Day 7: after surgery

Discussion

The Persian cat was distinguished and rare case reported as a breed predisposition to many rare diseases such as portosystemic shunts (Lipscomb et al., 2007). This case report, the cat demonstrated a congenital disease since the onset of the disease was starting at a very young age (3-year-old). The portosystemic shunts in cat were initially recognized by clinical signs of hypersalivation, seizure and head pressing, as a result from combination of factors such as hyperammonemia, oxidative stress, inflammation, and false neurotransmitter (Strickland et al., 2021). Hypersalivation has shown in the previous report (Strickland et al., 2021) as well as in this cat.

Laboratory tests are commonly used for diagnosis PSS include serum ammonia and bile acid stimulation test. Fasting ammonia is increase in majority of cats with PSS with 83% sensitivity and 76% specificity, while bile acid stimulation test has 100% sensitivity and specificity 71% (Ruland et al., 2009a). Ammonia is very labile and must be analysed in a short period (Carr 2007). The optimal time for test ammonia is 6 hours (Paepe et al., 2007). Bile acid should be measured in both preprandial-postprandial. Preprandial bile acid will be normal or low in serum, in contrary to postprandial bile acid which stimulated by food will be more than normal range in cat with PSS (Tivers and Lipscomb 2011a). In this report, serum ammonia from the first visit was done before fasting which could cause elevation of ammonia level as a result of the amino acid from dietary proteins producing most of the ammonia (Dimski 1994). However, after fasting the ammonia level was still higher than normal range. Bile acid is important to confirm PSS and the result was abnormal in this case.

Clinical signs should be confirmed with radiographic imaging techniques such as radiography, ultrasonography, and CT scan. First, radiography should not be used as the ultimate diagnosis or rule out PSS. Moreover, it cannot distinguish between acquired portosystemic shunts or congenital portosystemic shunts (Blaxter et al., 1988). Identification of portosystemic shunt

by ultrasonography can be difficult due to the present of gas in gastrointestinal tract, urolithiasis, and renomegaly could curtail the portosystemic shunts (Lamb et al., 1996). Nonetheless, the ultrasonography could reveal microhepatica with normal echogenicity. The ultrasonography was one clue technique to aid in diagnosis the porta hepatic (Leeman et al., 2013). However, it was unable to make a definitive diagnosis the PSS in this report. (Papamichail et al., 2018). Limitation was it required the specialist who experienced in using color and pulse Doppler (Lamb 1998). CT scan measurement has higher sensitivity and specificity than ultrasonography especially in cat. CT scan reported vessels of PSS in cat are gastroduodenal vein, a colonic vein, azygous vein (Blaxter et al., 1988; Cabassu et al., 2011). In this case report, left gastric vein was found and was considered as the most common type of extrahepatic portosystemic shunts similarly to the previous reports in Persian cat (Lipscomb et al., 2007).

There were two surgical procedures that could be performed in this case by using the ameroid constrictor and cellophane band. Ameroid constrictor in cat has a poor outcome and should be cautious after use (Lipscomb et al., 2007). Considering ameroid constrictor made from casein and stainless steel which encases a C shaped doughnut of casein, Casein will absorbs body fluid the ameroid ring constrictor to close to 42-48% and possibly induces risk of allowing continued shunting (Hunt et al., 2014). Furthermore, the ring is scrutinizing as a metal artifact which has a reaction with CT scan (Leeman et al., 2013). Cellophane, made from cellulose (McAlinden et al., 2010), does not effect with the CT imaging and have no tissue reaction from antibody. Survival rate was presented around 33-75 % (Valiente et al., 2020), but cellophane band is more effective method of alleviating hepatic dysfunction resulting from a congenital portosystemic shunt. Incident of life threatening portal hypertension was very low when using a cellophane band (Havig and Tobias 2002) and survival rate are reported as 66-100% (Valiente et al., 2020) the same as in this case report. Mostly in dog, another surgical option is vessel ligation but the prognosis is based on the degree of shunting and was considered out of date (Tillson and Winkler 2002b; Hunt et al., 2004a). Nevertheless, in cats survival rate ranged from 66-75% for this method (Valiente et al., 2020).

Duration of hospitalization was 7 days after surgery for close monitoring. Cats can develop refractory seizure (Cabassu et al., 2011). However, it was not found in this case. Postoperative seizure can be minimized with preoperative levetriracetam as a prevention Nonetheless, it did not prevent the occurrence of a further seizure. It was suggested that the dosage for levetrracetam is 20mg/kg every 6 hour during 24 hours preoperative period and continue for 5 days postoperation (Strickland et al., 2021). Some cats were euthanized after surgery in 90 days because of the uncontrolled seizure (Valiente et al., 2020). This case report has monitored the cat for more than 120 days and no seizure was observed. Ideally, a close monitor of shunt by a CT scan is very useful (Leeman et al., 2013) but limited in this case due to a financial issue. The authors decided to monitor with ultrasonography after surgery. Neurological signs were the only fatal postoperative concern which developing in 37% of cats (Lipscomb et al., 2007) within 3 days post operation. Other factors that also imperative are serum glucose, electrolyte and bile acid level (Greenhalgh et al., 2010).

Another disease with a similar clinical sign was a primary hypoplasia of portal vein but very rare in cats. The typical screening test was blood examination especially

ammonia and bile acid. For the histolopathology from liver biopsy can be used to confirm the acquired portosystemic shunts with the decreased of portal vein diameter or absence of the portal vein, number of arteriolar profiles are more than normal (Sugimoto et al., 2018). However, liver biopsy was not done in this case report because of that invasive diagnosis. Later hepatic disease in this study was rule out by relative noninvasive such as hematology and liver laboratory test. In dog, liver histopathology from liver biopsy led to detection of hepatic lipogranulomas (Isobe et al., 2008).

Conclusion

In this report, congenital portosystemic shunts in cats can be diagnosed not only by ultrasonography but also by CT scan. A serum ammonia levels is required as well as serum bile acid test. Thus, cellophane band of surgery is an ideal way for surgical procedure that supporting the previous reports. Seizures can be occurred before, during, or after surgery, and is mostly the cause of mortality. The owner's dedication is supporting the diagnosis, surgery, and postoperative care of PSS. The major limitation in this case was lacked of hepatic histopathology and limited postoperative gold standard CT scan to confirm shunt closure.

Acknowledgements

The authors would like to express their sincere gratitude to all staffs at Prasuarthon Animal Hospital with the owner permission and this patient whose support and collaboration made this case report possible.

References

Berent AC, Tobias KM. Portosystemic Vascular Anomalies. Veterinary Clinics of North America: J Small Anim Pract. 2009;39(3):513-41.

Blaxter AC, Holt PE, Pearson GR, Gibbs C, Gruffydd-Jones TJ. Congenital portosystemic shunts in the cat: A report of nine cases. J Small Anim Pract. 1988;29(10):631-45.

Buob S, Johnston AN, Webster CR. Portal hypertension: pathophysiology, diagnosis, and treatment. J Vet Intern Med. 2011;25(2):169-86.

Cabassu J, Seim HB, 3rd, MacPhail CM, Monnet E. Outcomes of cats undergoing surgical attenuation of congenital extrahepatic portosystemic shunts through cellophane banding: 9 cases (2000-2007). J Am Vet Med Assoc. 2011;238(1):89-93.

Carr AP. 42 - Liver. In: Rubin SI, Carr AP, editors. Canine Internal Medicine Secrets. Saint Louis: Mosby; 2007. p. 293-304.

Devriendt N, Serrano G, Paepe D, de Rooster H. Liver function tests in dogs with congenital portosystemic shunts and their potential to determine persistent shunting after surgical attenuation. Vet J. 2020;261:105478.

Dimski DS. Ammonia metabolism and the urea cycle: function and clinical implications. J Vet Intern Med. 1994;8(2):73-8.

Greenhalgh S, Dunning M, McKinley T, Goodfellow M, Kelman K, Freitag T, et al. Comparison of survival after surgical or medical treatment in dogs with a congenital portosystemic shunt. J Am Vet Med Assoc. 2010;236:1215-20.

Havig M, Tobias KM. Outcome of ameroid constrictor occlusion of single congenital extrahepatic portosystemic shunts in cats: 12 cases (1993-2000). J Am Vet Med Assoc. 2002;220(3):337-41.

Hunt GB, Kummeling A, Tisdall PL, Marchevsky AM, Liptak JM, Youmans KR, et al. Outcomes of cellophane banding for congenital portosystemic shunts in 106 dogs and 5 cats. Vet Surg. 2004a; 33(1):25-31.

Hunt GB, Culp WT, Mayhew KN, Mayhew P, Steffey MA, Zwingenberger A. Evaluation of in vivo behavior of ameroid ring constrictors in dogs with congenital extrahepatic portosystemic shunts using computed tomography. Vet Surg. 2014b;43(7):834-42.

Isobe K, Matsunaga S, Nakayama H, Uetsuka K. Histopathological characteristics of hepatic lipogranulomas with portosystemic shunt in dogs. J. Vet. Med. Sci. 2008;70(2):133-8.

Joffe MR, Hall E, Tan C, Brunel L. Evaluation of different methods of securing cellophane bands for portosystemic shunt attenuation. Vet Surg. 2019; 48(1):42-9.

Lamb CR, Forster-van Hijfte MA, White RN, McEvoy FJ, Rutgers HC. Ultrasonographic diagnosis of congenital portosystemic shunt in 14 cats. J Small Anim Pract. 1996;37(5):205-9.

Lamb CR. Ultrasonography of Portosystemic Shunts in Dogs and Cats. Vet Clin North Am†Small Anim Pract. 1998;28(4):725-53.

Leeman JJ, Kim SE, Reese DJ, Risselada M, Ellison GW. Multiple congenital PSS in a dog: case report and literature review. J Am Anim Hosp Assoc. 2013;49(4):281-5.

Lipscomb VJ, Jones HJ, Brockman DJ. Complications and long-term outcomes of the ligation of congenital portosystemic shunts in 49 cats. Vet Rec. 2007; 160(14):465-70.

McAlinden AB, Buckley CT, Kirby BM. Biomechanical evaluation of different numbers, sizes and placement configurations of ligaclips required to secure cellophane bands. Vet Surg. 2010;39(1):59-64.

Paepe D, Vermote K, Saunders J, Risselada M, Daminet S. Portosystemic shunts in dogs and cats: Laboratory diagnosis of congenital portosystemic shunts. Vlaams Diergeneeskd. Tijdschr. 2007;76:241-8.

Papamichail M, Pizanias M, Heaton N. Congenital portosystemic venous shunt. Eur J Pediatr. 2018; 177(3):285-94.

Ruland K, Fischer A, Hartmann K. Sensitivity and specificity of fasting ammonia and serum bile acids in the diagnosis of portosystemic shunts in dogs and cats. ASVCP. 2009a;39:57-64.

Ruland K, Fischer A, Reese S, Zahn K, Matis U, Hartmann K. Portosystemic shunts in cats-evaluation of six cases and a review of the literature. Berl Munch Tierarztl Wochenschr. 2009b;122(5-6):211-8.

Strickland R, Tivers MS, Fowkes RC, Lipscomb VJ. Incidence and risk factors for neurological signs after attenuation of a single congenital portosystemic shunt in 50 cats. Vet Surg. 2021;50(2):303-11.

Sugimoto S, Maeda S, Tsuboi M, Saeki K, Chambers JK, Yonezawa T, et al. Multiple acquired portosystemic shunts secondary to primary hypoplasia of the portal vein in a cat. J Vet Med Sci. 2018;80(6):874-7.

Tillson DM, Winkler JT. Diagnosis and treatment of portosystemic shunts in the cat. Vet Clin North Am Small Anim Pract. 2002;32(4):881-99.

Tivers M, Lipscomb V. Congenital Portosystemic Shunts in Cats: Investigation, diagnosis and stabilisation. J Feline Med Surg. 2011a;13(3):173-84.

Tivers M, Lipscomb V. Congenital Portosystemic Shunts in Cats: Surgical management and prognosis. J Feline Med Surg. 2011b;13(3):185-94.

Tobias KM. Current veterinary therapy. St louis (MO): Saunders Elsevier; 2009.

Valiente P, Trehy M, White R, Nelissen P, Demetriou J, Stanzani G, et al. Complications and outcome of cats with congenital extrahepatic portosystemic shunts treated with thin film: Thirty-four cases (2008-2017). J Vet Intern Med. 2020;34(1):117-24.

Research Articles

A Preliminary In Vitro Study on the Effect of Zika Virus Strains on the Quality of Boar Sperm

Natnicha Payomthip[1] Thamonwan Panduang[1] Warinthorn Aimsan[1]
Warunya Chakritbudsabong[2] Panida Chanapiwat[3,4] Kampon Kaeoket[3,4]
Sasitorn Rungarunlert[2*]

[1]Sixth year student, Faculty of Veterinary Science, Mahidol University, Nakhon Pathom, Thailand
[2]Department of Pre-clinic and Applied Animal Science, Faculty of Veterinary Science, Mahidol University, Nakhon Pathom, Thailand
[3]Department of Clinical Sciences and Public Health, Faculty of Veterinary Science, Mahidol University, Nakhon Pathom, Thailand
[4]Semen Laboratory, Faculty of Veterinary Science, Mahidol University, Nakhon Pathom, Thailand

[*]Corresponding author, E-mail address: sasitorn.run@mahidol.edu

Received: 6 July 2022; Revised: 31 August 2022; Accepted: 7 September 2022

Abstract

A million people in various countries have been infected by the Zika virus (ZIKV). Sexual transmission is one of the human infectious transmissions. ZIKV causes neurological disease and microcephaly in infants whose mothers have been infected. Domestic pigs were used as an experimental model because the symptoms of ZIKV-infected piglets are similar to humans. Nowadays, minimal evidence of ZIKV infection in boar semen has been published, and there is no data on the effect of ZIKV strains. Thus, this study compares the quality of boar semen infected by different ZIKV strains. The fresh semen from two boars were collected by gloved-hand technique. The quality of the semen was determined and it was separated into three groups: a non-infected semen (mock) group, and two ZIKV-infected semen groups (strains SV0010/15, and SV0127/14). Then, at 2, 24, 48, and 72 hours after infection, the sperm viability and acrosomal integrity were assessed using Eosin-nigrosin and FITC-PNA, respectively. The morphology of head and tail sperms was determined using Williamís stain and formal saline, respectively. The results indicated that there were no significant differences in the quality of boar semen between groups ($P > 0.05$), but that sperm head and tail abnormalities trended to be increased overtime in all groups. In conclusion, the boar sperm may be not a target cell of ZIKV. Thus, additional samples for further research on the ZIKV receptor in sperm should be acquired.

Keywords: Zika virus, pigs, sperm, strains

การศึกษาเบื้องต้นในหลอดทดลองเกี่ยวกับผลของสายพันธุ์ของเชื้อไวรัสซิกาต่อคุณภาพอสุจิสุกร

ณัฐณิชา โพยมทิพย์[1] ธมนวรรณ ปานดวง[1] วรินทร เอมสรรค์[1]
วรัญญา ชาคริตบุษบง[2] พนิดา ชนาภิวัฒน์[3,4] กัมพล แก้วเกษ[3,4] ศศิธร รุ่งอรุณเลิศ[2*]

[1]นักศึกษาชั้นปีที่ 6 คณะสัตวแพทยศาสตร์ มหาวิทยาลัยมหิดล ตำบลศาลายา อำเภอพุทธมณฑล จังหวัดนครปฐม
[2]ภาควิชาปรีคลินิกและสัตวศาสตร์ประยุกต์ คณะสัตวแพทยศาสตร์ มหาวิทยาลัยมหิดล ตำบลศาลายา อำเภอพุทธมณฑล จังหวัดนครปฐม
[3]ภาควิชาเวชศาสตร์คลินิกและการสาธารณสุข คณะสัตวแพทยศาสตร์ มหาวิทยาลัยมหิดล ตำบลศาลายา อำเภอพุทธมณฑล จังหวัดนครปฐม
[4]ศูนย์ตรวจวินิจฉัยทางการสัตวแพทย์ ห้องปฏิบัติการวิทยาการสืบพันธุ์ คณะสัตวแพทยศาสตร์
มหาวิทยาลัยมหิดล ตำบลศาลายา อำเภอพุทธมณฑล จังหวัดนครปฐม

[*]ผู้รับผิดชอบบทความ E-mail address: sasitorn.run@mahidol.edu

Received: 6 July 2022; Revised: 31 August 2022; Accepted: 7 September 2022

บทคัดย่อ

การระบาดของโรคติดเชื้อไวรัสซิกาได้มีการแพร่กระจายเชื้อในหลายประเทศ ส่งผลให้มีผู้ติดเชื้อจำนวนมาก การติดต่อทางเพศสัมพันธ์เป็นทางหนึ่งที่ทำให้ติดเชื้อไวรัสซิกาในมนุษย์ ไวรัสซิกาเป็นสาเหตุที่ทำให้เกิดโรคทางระบบประสาทและทารกมีศีรษะขนาดเล็กจากแม่ที่ติดเชื้อขณะตั้งครรภ์ สุกรถูกใช้เป็นโมเดลในงานทดลอง เนื่องจากลูกสุกรที่ติดเชื้อไวรัสซิกามีอาการเช่นเดียวกับในมนุษย์ ในปัจจุบันมีหลักฐานเกี่ยวกับการติดเชื้อไวรัสซิกาในอสุจิสุกรน้อย และไม่พบการรายงานถึงผลของสายพันธุ์ไวรัสซิกา ดังนั้นงานวิจัยนี้จึงศึกษาความแตกต่างของสายพันธุ์ไวรัสซิกาต่อคุณภาพอสุจิสุกร โดยการทดลองครั้งนี้จะใช้น้ำเชื้อสดที่รีดมาจากพ่อสุกรจำนวน 2 ตัว ซึ่งน้ำเชื้อสดที่ได้มีการประเมินคุณภาพน้ำเชื้อก่อนทำการทดลอง และแบ่งน้ำเชื้อออกเป็น 3 กลุ่มได้แก่ กลุ่มที่ไม่ติดเชื้อ (mock) และกลุ่มที่ติดเชื้อไวรัสซิกา 2 กลุ่ม (สายพันธุ์ SV0010/15 และ สายพันธุ์ SV0127/14) จากนั้นที่เวลา 2, 24, 48 และ 72 ชั่วโมงหลังติดเชื้อไวรัสซิกา ได้ทำการตรวจประเมินคุณภาพน้ำเชื้อ ได้แก่ อัตราการมีชีวิตรอดของตัวอสุจิ และความสมบูรณ์ของอะโครโซม ด้วยวิธี Eosin-nigrosin และ FITC-PNA ตรวจประเมินความผิดปกติของอสุจิส่วนหัวและหาง ด้วยวิธี William's stain และ formal saline ตามลำดับ ผลการทดลองพบว่าคุณภาพน้ำเชื้อสุกรระหว่างกลุ่มการทดลองไม่มีความแตกต่างกันอย่างมีนัยสำคัญทางสถิติ ($P > 0.05$) แต่เมื่อเวลาผ่านไปพบความผิดปกติที่ส่วนหัวและหางของอสุจิในทุกกลุ่มการทดลองมีแนวโน้มเพิ่มสูงขึ้น สรุปได้ว่าอสุจิสุกรอาจจะไม่ใช่เป้าหมายของไวรัสซิกา ดังนั้นสำหรับการศึกษาวิจัยในอนาคตควรมีการตรวจหาตัวรับของอสุจิเพิ่มเติม

คำสำคัญ : ไวรัสซิกา สุกร อสุจิ สายพันธุ์

Introduction

The Zika virus (ZIKV) has infected millions of people since it first emerged in the Americas. The virus has spread to many parts of the world, including Africa, the Americas, Asia, and the Pacific. The spread of ZIKV has increased, raising public health concerns and necessitating increased surveillance (Lazear and Diamond 2016). The Thailand report during the 2012-2014 outbreak investigation into public health. Seven cases of acute infection were discovered in Ratchaburi, Lamphun, Sisaket, and Phetchabun (Buathong et al., 2015). ZIKV is primarily transmitted via the human-mosquito-human transmission cycle, predominantly by Aedes mosquitoes, but it is also transmitted via non-mosquito transmission, including sexual transmission, mother-to-fetus transmission, and blood transfusion (Petersen et al., 2016; Agumadu and Ramphul 2018). The three clinical aspects of ZIKV infection are as follows: (1) acute febrile illness, with 90% of patients developing a macular or papular rash; (2) neurological complications, such as Guillain-Barré syndrome and meningoencephalitis; and (3) adverse fetal outcomes, such as congenital anomalies associated with maternal rubella infection during pregnancy (Petersen et al., 2016).

The ZIKV genome is a single-stranded positive-sense RNA from the family Flaviviridae that encodes three structural proteins (C, prM, and E) and seven non-structural proteins (NS1, NS2A, NS2B, NS3, NS4A, NS4B, and NS5). The ZIKV is categorized into two major lineages: African and Asian/American. The mutations in prM and NS1 were associated with differences in pathogenicity in mice, viral protein antigenemia, and interferon stimulation in host cells between Asian and American-lineage strains (Kawai et al., 2019). In Thailand, SV0010/15 and SV0127/14 were isolated from the blood of patients (Ellison et al., 2016; Sornjai et al., 2018). Non-structural proteins, which are required for flavivirus replication, are the difference between these strains. As a result, these strains differ in terms of infection and cell tropism (Rastogi et al., 2016; Klaitong and Smith 2021). ZIKV was detected in seminal plasma and semen cells (Joguet et al., 2017; Calvet et al., 2018) and was found to be localized in the head of human spermatozoa using immunofluorescent staining (Joguet et al., 2017).

Domestic pigs are anatomically, physiologically, genetically, and immunologically similar to humans, making them an ideal animal model for studying a variety of human viral diseases, particularly ZIKV (Darbellay et al., 2017). According to a previous report, one-day-old piglets were susceptible to ZIKV infection. Neonatal pigs were intracerebrally injected with ZIKV strain PRVABC59. This strain was isolated from a human serum in Puerto Rico in 2015. Two out of eleven piglets had limb weakness, ataxia, and tremor (Darbellay et al., 2017). Moreover, another report showed that microencephaly in fetal piglets infected with ZIKV via intrauterine injection at mid-gestion was associated with neuronal depletion in the cerebral cortices of several lobes in all fetuses (Wichgers Schreur et al., 2018). To have a better understanding of sexual transmission, boar sperm infected with ZIKV was used as an animal model. This report was confirmed to be incapable of ZIKV replication due to the fact that viral RNA levels decreased considerably with increasing time post infection. Sperm morphology remained unchanged significantly. Transmission electron microscopy detected virus-free sperm, indicating that ZIKV cannot replicate in boar sperm. This phenomenon could be caused by at least three factors, including boar spermatozoa may not be a target of ZIKV, ZIKV replication may be affected by the environment of spermatozoa, and ZIKV may not be

spermatozoa tropism (Luplertlop et al., 2017). There was no study that investigated the impact of the ZIKV strains on boar sperm quality. Hence, the purpose of this study was to determine the influence of two ZIKV strains (SV0010/15 vs. SV0127/14) on boar sperm quality.

Materials and Methods

1. Animal

The experimental animal was evaluated and approved by the Institutional Animal Care and Use Committee at Faculty of Veterinary Science, Mahidol University in Thailand (Approval ID: MUVS-2020-06-16). Two Duroc boars, aged 1-3 years old, were kept in individual pens in an evaporative housing system. Animals were fed twice a day with commercial feed, and water was provided ad libitum. The boars had confirmed sperm quality and were used for regular artificial insemination (AI) (Chanapiwat and Kaeoket 2015).

2. Collection and preparation of semen

The collection technique was a gloved-hand technique by worker in farm. Within 20 minutes, volume, concentration, sperm motility, sperm viability, and acrosomal integrity were all evaluated (Chanapiwat and Kaeoket 2015). Then, the semen was diluted in BTS extender 1:1 v/v and incubated at 18°C (Chanapiwat and Kaeoket 2021).

3. Semen evaluation

3.1 Semen volume

The volume of the boar semen was measured by the cylinder. A normal boar semen volume is 150-500 ml.

3.2 Sperm motility

The computer-assisted sperm analysis, CASA (Hamilton Thorne Biosciences, version 12 TOX VIOS, Beverly, USA), was used to evaluate the total motility and progressive motility. Seven µl of semen were pipetted into a pre-warmed (37°C) glass slide and measured at 10x magnification. At least five different fields or 600 sperm were evaluated (Ratchamak et al., 2019).

3.3 Sperm viability

The sperm was stained with Eosin-nigrosin, and two hundred spermatozoa were examined under a microscope at 400x magnification. Sperm viability was calculated as the percentage of alive spermatozoa. Normal sperm viability is more than 80% (Buranaamnuay 2019).

3.4 Acrosomal integrity

Fluorescein isothiocyanate-labeled peanut (Arachis hypogaea) agglutinin (FITC-PNA) staining was used to assess acrosomal integrity. Diluted semen was mixed with Ethidiumhomodimer-1 and incubated at 37°C for 15 minutes. The mixture was smeared on a glass slide and fixed with 95% ethanol for 30 seconds. FITC-PNA (diluted FITC-PNA with PBS 1:10 v/v) was spread over the slide and incubated in a moist chamber at 4°C for 30 minutes. After incubation, the slides were rinsed with cold PBS and air dried.One hundred spermatozoa were assessed under fluorescent microscope at 400x magnification and calculated as a percentage of intact acrosome (Chanapiwat and Kaeoket 2015).

3.5 Sperm abnormality

There were two tests for sperm abnormality, including head abnormality and tail abnormality. The sperm head abnormality was tested by William's stain. Sperm was placed thinly over a glass slide and air dried. The slide was dipped in alcohol and dried by air. The slide was then immersed in a 0.5% Chloramine-T solution, rinsed in distilled water, and soaked in 95% alcohol. Then, the slide was stained with Carbol-fuchsin dye, washed with distilled water, and air dried again. Two hundred

spermatozoa were assessed under the light microscope at 400x magnification and recorded the percentage of head abnormality of spermatozoa. The example of sperm head morphology was shown in Figure 1. The sperm tail abnormality was examined by mixing of sperm and formal saline. Two hundred spermatozoa were assessed under light microscope at 400x magnification and recorded the percentage of tail abnormality of spermatozoa. The example of sperm tail morphology was shown in Figure 2 (Kaeoket et al., 2010).

3.6 Sperm concentration

The concentration of sperm was determined using a Neubauer hemocytometer at dilution of the sperm with formal saline at a ratio of 1:100 v/v. The sperm were examined under microscopy at 400x magnification and the calculation for sperm concentration was 30 x 10^6 sperm/ml (Kaeoket et al., 2010).

4. Preparation of ZIKV

The ZIKV strains (SV0010/15 and SV0127/14) were received from the Monitoring and Surveillance Center for Zoonotic Disease in Wildlife and Exotic Animals (MoZWE), Faculty of Veterinary Science, Mahidol University. Both strains of the ZIKV were propagated in African Green Monkey Kidney cells (Vero cells) with DMEM (Dulbecco's Modified Eagle Medium) and 2% fetal bovine serum and incubated in a cell culture incubator. Infected cells were noticed for viral cytopathic effects at 6, 24, and 48 hours after infection. Centrifugation was used to remove cell debris from the supernatant. Plaque assays on a Vero cell monolayer were used to determine the ZIKV titers in the culture supernatants, which were represented as plaque-forming units (PFU). As with the ZIKV stocks, the culture supernatant was aliquoted and kept at 80°C until needed.

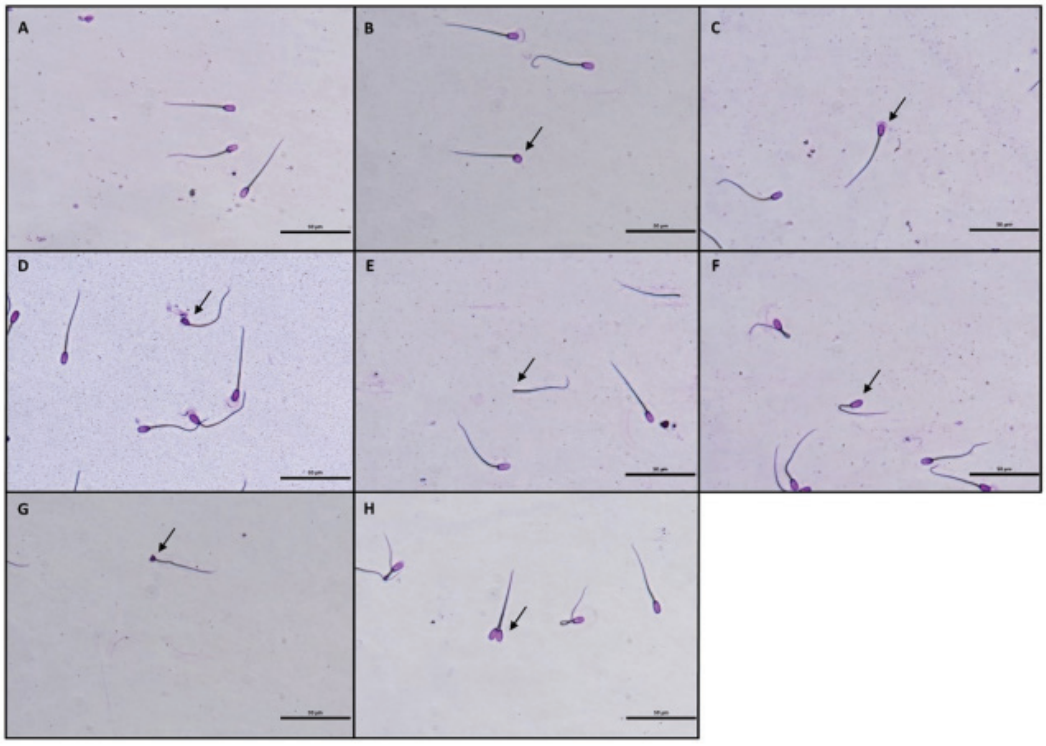

Figure 1. The light microscopy of sperm head morphology, as indicated by William's staining. (A) Normal head (B) Round head (C) Additional cap (D) Microcephalic (E) Loose head (F) Macrocephalic (G) Acrosomal defect (H) Double head.

Prior to conducting the experiment, the plaque assay findings were used to calculate the multiplicity of infection (MOI). The results were averaged and calculated for MOI. Finally, the MOI was 0.3 (Horcharoensuk et al., 2022).

5. Infection of semen with ZIKV and post-infection sample harvesting

The boar semen samples were infected with ZIKV (SV0010/15 and SV0127/14) at 10 x 10^6 pfu/ml (MOI = 0.3) with 30 x 10^6 sperm/ml as the treatment groups. Both these groups and the mock (control) group were incubated at 18°C for 2 hours (Luplertlop et al., 2017). Then, semen samples were centrifuged at 2,000 rpm at 18°C for 5 minutes to remove the supernatant. Finally, the treatment groups were added 1.2 ml of BTS extender, and all groups were harvested at 2, 24, 48, and 72 hours after infection for analysis sperm viability, acrosomal integrity, and sperm abnormality.

6. Data analysis and statistical method

Each experiment was repeated at least three times. The data was analyzed using SPSS version 22. The statistical data for sperm viability, acrosomal integrity, and sperm abnormalities were expressed as mean ± SD. The Shapiro-Wilk test was used to determine the normal distribution of all parameters. A one-way analysis of variance was used to determine the statistical significance of the differences between groups (one-way ANOVA). P value < 0.05 was considered a significant difference.

Results

In total, two semen samples from two boars were collected for this study. We evaluated boar sperm prior to infection with ZIKV as shown in Table 1.

Evaluation of boar semen after post-ZIKV infection

The post-ZIKV infection was examined for sperm viability, acrosomal integrity, and abnormalities in morphology.

Sperm viability

The results of sperm viability revealed no statistically significant differences among the SV0127/14 group, SV0010/15 group, and mock group at 2, 24, 48, and 72 hours post infection ($P > 0.0$ 5) (Figure 3).

Acrosomal integrity

The results of sperm acrosomal integrity revealed no statistically significant differences among the SV0127/14 group, SV0010/15 group, and mock group at 2, 24, 48, and 72 hours post infection (P > 0.05) (Figures 3 and 4).

Sperm abnormality

The results of sperm head and tail abnormalities revealed no statistically significant difference among the SV0127/14 group, SV0010/15 group, and mock group at 2, 24, 48, and 72 hours post infection ($P > 0.05$). However, as time passed after infection, the trend of sperm head and tail abnormalities increased in all groups. The 7 types of sperm head abnormalities and 8 types of sperm tail abnormalities were shown in Figures 1 and 2, respectively. The percentage of each type is shown in Table 2.

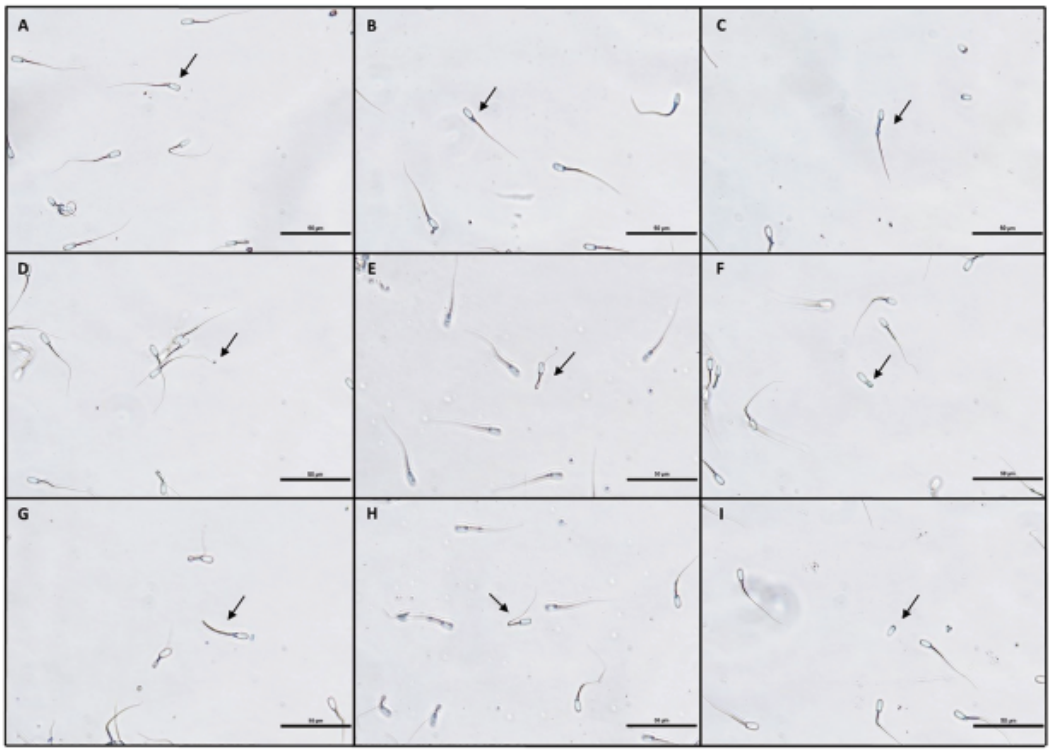

Figure 2. The light microscopy of sperm tail morphology. (A) Normal tail (B) Proximal protoplasmic droplet (C) Distal protoplasmic droplet (D) Terminal droplet (E) Folded tail (F) Coiled tail (G) Short tail (H) Bent tail (I) Loose tail.

Table 1. Descriptive statistics of semen parameters of boars pre-ZIKV infection.

Variables	N	Mean ± SD	Range
Semen volume (ml)	2	154.00±25.46	172.00-136.00
Sperm concentration (x10^6 sperm/ml)	2	467.70±60.39	510.40-425.00
Total motility (%)	2	88.23±0.98	88.92-87.53
Progressive motility (%)	2	83.86±0.40	83.58-84.14
Viability (%)	2	90.25±0.35	90.00-90.50
Acrosomal integrity (%)	2	87.00±2.83	85.00-89.00

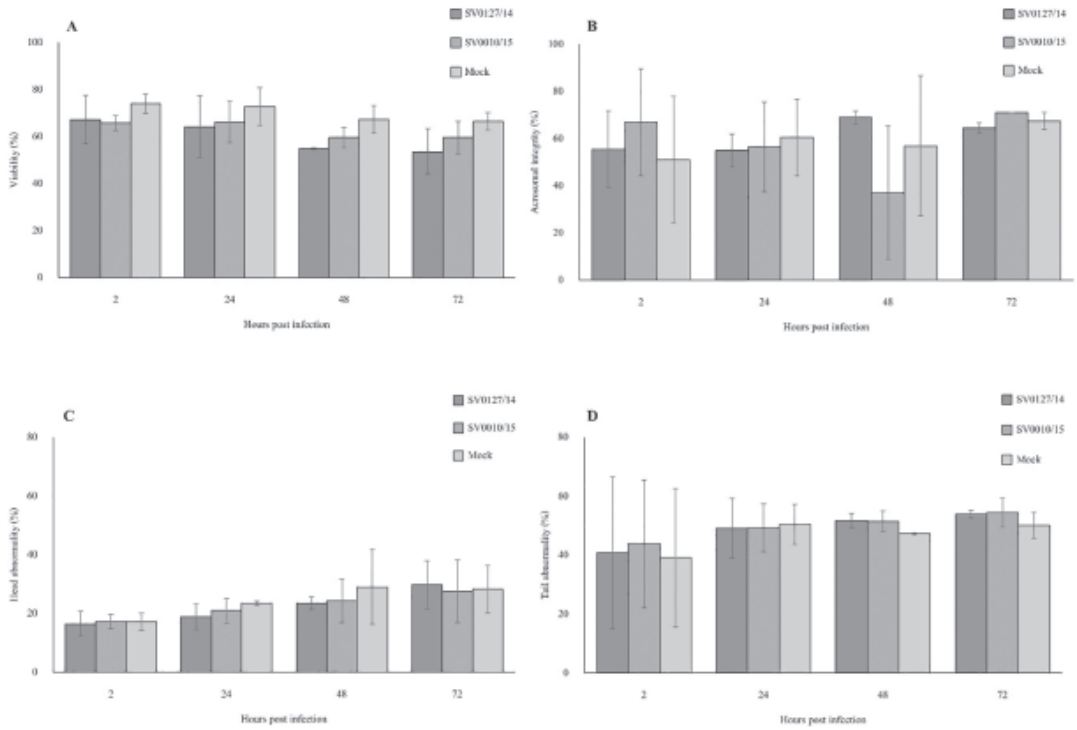

Figure 3. The effect of ZIKV infection on sperm quality in the SV0127/14, SV0010/15, and mock groups at 2, 24, 48, and 72 hours after infection. (A) Sperm viability (%) (B) Acrosomal integrity (%) (C) Sperm head abnormality (%) (D) Sperm tail abnormality (%).

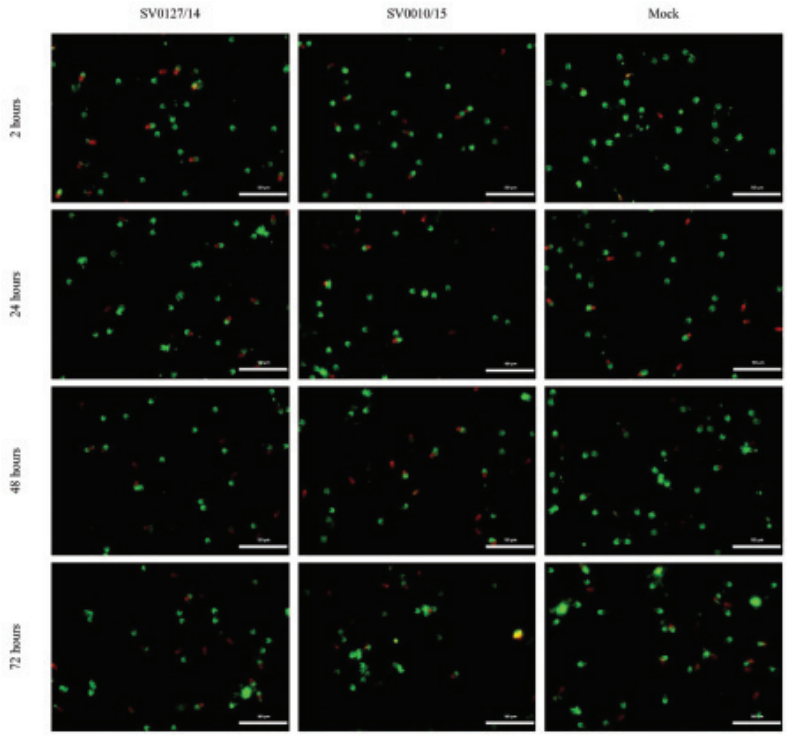

Figure 4. Sperm acrosomal integrity between the SV0127/14 group, SV0010/15 group, and mock group at 2, 24, 48, and 72 hours post infection using fluorescein isothiocyanateñlabeled peanut (Arachis hypogaea) agglutinin (FITC-PNA) staining.

Table 2. A descriptive statistic on the sperm defect of boar spermatozoa with different head abnormalities and tail abnormalities.

Sperm defect (%)	SV0127/14				SV0010/15				Mock			
	Hours post infection				Hours post infection				Hours post infection			
	2	24	48	72	2	24	48	72	2	24	48	72
Head defect												
Acrosomal defect	2.75±3.89	10.75±8.13	14.88±0.18	15.00±5.66	7.75±3.18	10.25±7.42	12.00±2.83	16.75±9.55	11.38±2.65	15.00±0.00	18.63±6.19	18.63±4.77
Round head	9.00±6.36	4.25±1.77	6.25±5.30	12.50±2.83	4.25±1.77	5.00±4.24	9.13±7.60	6.88±4.42	3.38±0.53	5.88±3.01	7.38±5.13	6.63±3.36
Microcephalic	0.25±0.35	0.50±0.71	0.25±0.35	0.75±1.06	0.50±0.71	1.00±1.41	0.50±0.71	0.88±0.53	1.50±1.41	0.63±0.88	0.00±0.00	0.38±0.53
Double head	0.00±0.00	0.00±0.00	0.00±0.00	0.25±0.35	0.00±0.00	0.38±0.18	0.00±0.00	0.00±0.00	0.00±0.00	0.00±0.00	0.13±0.18	0.00±0.00
Loose head	1.25±1.77	1.38±1.94	0.75±1.06	4.00±?3.54	0.88±1.24	1.88±2.65	1.25±0.35	1.63±0.88	0.25±0.35	0.75±0.35	2.50±2.12	2.00±1.41
Additional cap	3.00±4.24	1.75±2.47	1.38±1.94	3.75±5.30	3.38±4.77	2.38±3.36	1.38±1.94	1.38±1.94	0.00±0.00	1.13±1.59	0.38±0.53	0.63±0.88
Macrocephalic	0.25±0.35	0.25±?0.35	0.00±0.00	0.00±0.00	0.50±0.71	0.13±0.18	0.00±0.00	0.00±0.00	0.63±0.88	0.13±0.18	0.00±0.00	0.00±0.00
Tail defect												
Proximal protoplasmic droplet	5.13±7.25	7.00±0.71	7.25±3.18	7.50±4.24	6.25±3.89	7.00±3.54	6.38±2.65	8.75±1.77	8.00±3.54	7.38±4.07	7.25±1.06	8.38±4.77
Distal protoplasmic droplet	9.88±9.72	19.00±2.83	20.38±5.13	25.00±11.31	17.00±6.36	21.63±4.07	23.75±10.25	23.75±7.42	14.00±7.78	22.75±8.13	21.38±13.61	22.25±10.25
Terminal droplet tail	1.00±0.71	0.75±1.06	0.63±0.18	0.13±0.18	0.50±0.00	0.50±0.71	0.00±0.00	0.50±0.71	0.38±0.53	0.63±0.88	0.88±1.24	0.50±0.71
Folded tail	21.50±8.49	18.88±11.84	20.25±2.47	18.00±9.90	17.50±12.02	15.88±7.60	16.50±14.85	18.25±10.25	15.00±11.31	18.50±9.90	16.38±11.14	16.25±10.96
Coiled tail	0.50±0.71	1.75±1.77	0.88±0.53	0.50±0.71	0.38±0.53	1.13±0.53	1.38±0.18	1.88±0.88	0.75±0.35	0.50±0.00	0.38±0.53	0.13±0.18
Short tail	0.38±0.53	0.75±?0.35	0.50±0.00	1.38±1.59	0.63±0.53	1.13±0.53	0.75±0.35	0.25±0.35	0.63±0.18	0.38±0.18	0.25±0.35	1.13±1.24
Bent tail	1.00±0.71	0.88±0.53	1.13±0.18	1.25±1.06	1.38±0.88	1.38±0.53	2.50±3.54	0.50±0.00	0.25±0.35	0.13±0.18	1.00±1.41	0.75±1.06
Loose tail	1.38±1.94	0.13±0.18	0.38±0.53	0.13±0.18	0.25±0.35	0.63±0.88	0.25±0.35	0.63±0.88	0.13±0.18	0.13±0.18	0.25±0.35	0.75±0.35

Discussion

The sexual transmission of ZIKV is a significant concern, especially for pregnant women and couples getting pregnant, due to the serious consequences of ZIKV infection during pregnancy. Numerous case reports have demonstrated ZIKV shedding in the semen of symptomatic and asymptomatic humans (Joguet et al., 2017). The infectivity of ZIKV in reproductive systems has been studied using boar sperm as a model. However, there has been one study on ZIKV sexual transmission in boar sperm (Luplertlop et al., 2017). Our study showed that the quality of spermatozoa did not change significantly between mock and ZIKV-infected groups (strains SV0010/15 and SV0127/14). Moreover, similar to Luplertlop et al. (2017), our study found no significant alterations in sperm morphology. This could be attributed to the minimal number of samples included in our analysis and the lack of receptor detection. According to a previous report, the viral persistence in sperm was a major concern and could be linked to a viral tropism for male sexual cells (Mansuy et al., 2016). On the other hand, spermatozoa do not express the potential ZIKV entry Axl receptor in their heads. Sertoli cells have a high level of Axl expression and play an important role in spermatogenesis. According to another study, ZIKV can infect human testicular tissue and replicate in human Sertoli cells (Rastogi et al., 2020). Furthermore, Da Silva, (2018), reported that of ZIKV trafficking and interactions in the human male reproductive tract, found that ZIKV infection can affect male fertility by altering specific stages of the seminiferous epithelial cycle, resulting in a decrease in total sperm count, as has already been reported in long-term shedders of this virus in semen (Da Silva 2018). Moreover, ZIKV was found primarily in the mid-piece of mature spermatozoa, indicating that Tyro3 receptors, which were largely expressed on the mid-piece of human spermatozoa, were involved in ZIKV binding and entry (Bagasra et al., 2017).

Conclusions

In conclusion, our results back up the hypothesis that ZIKV may not infect boar sperm, but sperm defect rates trend upward.†It is possible that sperm boar may not be a ZIKV target, or that ZIKV may not be a cell tropism for spermatozoa. Further study is necessary to collect more samples and should be studied in vivo to fully understand the mechanism of ZIKV transmission to cells during spermatogenesis. To understand the relationship between sexual transmission and viruses, ZIKV may infect other cells such as Leydig cells, Sertoli cells, and seminiferous epithelial cells. Moreover, in further study should detect ZIKV receptors on spermatozoa to understand the ZIKV target and real-time RT-PCR should be determined for viral RNA detection to proof that ZIKV was remained.

Acknowledgements

This study was financially supported by Faculty of Veterinary Science, Mahidol University. We gratefully thank Asst. Prof. Dr. Sarin Suwanpakdee for advice in the statistical analysis, Miss Jarupha Taowan for ZIKV propagation, and Dr. Pirom Prompiram for their technical assistant; Faculty of Veterinary Science, Mahidol University.

References

Agumadu VC, Ramphul K. Zika virus: A review of literature. Cureus. 2018;10(7):e3025.

Bagasra O, Addanki KC, Goodwin GR, Hughes BW, Pandey P, McLean E. Cellular targets and receptor of sexual transmission of zika virus. Appl Immunohistochem Mol Morphol. 2017;25(10): 679-86.

Buathong R, Hermann L, Thaisomboonsuk B, Rutvisuttinunt W, Klungthong C, Chinnawirotpisan P, et al. Detection of zika virus infection in Thailand, 2012-2014. Am J Trop Med Hyg. 2015;93(2):380-3.

Buranaamnuay K. Comparison of different methods for sperm vitality assessment in frozen-thawed Holstein bull semen. Thai J Vet Med. 2019;49(3): 249-55.

Calvet GA, Kara EO, Giozza SP, B?tto-Menezes CHA, Gaillard P, de Oliveira Franca RF, et al. Study on the persistence of Zika virus (ZIKV) in body fluids of patients with ZIKV infection in Brazil. BMC Infect Dis. 2018;18(1):49.

Chanapiwat P, Kaeoket K. l-cysteine prolonged fresh boar semen qualities, but not for docosahexaenoic acid. Czech J Anim Sci. 2021;66(1):21-8.

Chanapiwat P, Kaeoket K. The effect of Curcuma longa extracted (curcumin) on the quality of cryopreserved boar semen. Anim Sci J. 2015;86(9):863-8.

Da Silva LRC. Zika virus trafficking and interactions in the human male reproductive tract. Pathogens. 2018;7(2):51.

Darbellay J, Lai K, Babiuk S, Berhane Y, Ambagala A, Wheler C, et al. Neonatal pigs are susceptible to experimental Zika virus infection. Emerg Microbes Infect. 2017;6(2):e6.

Ellison DW, Ladner JT, Buathong R, Alera MT, Wiley MR, Hermann L, et al. Complete genome sequences of zika virus strains isolated from the blood of patients in Thailand in 2014 and the Philippines in 2012. Genome Announc. 2016;4(3):e00359-16.

Horcharoensuk P, Yang-en S, Chakritbudsabong W, Samatiwat P, Pramong R, Rungarunlert S, et al. Melatonin attenuates dimethyl sulfoxideñ and zika virusñinduced degeneration of porcine induced neural stem cells. In Vitro Cell Dev Biol Anim. 2022;58(3):232-42.

Joguet G, Mansuy JM, Matusali G, Hamdi S, Walschaerts M, Pavili L, et al. Effect of acute zika virus infection on sperm and virus clearance in body fluids: a prospective observational study. Lancet Infect Dis. 2017;17(11):1200-8.

Kaeoket K, Chanapiwat P, Tummaruk P, Techakumphu M. Supplemental effect of varying L-cysteine concentrations on the quality of cryopreserved boar semen. Asian J Androl. 2010;12(5):760-5.

Kawai Y, Nakayama E, Takahashi K, Taniguchi S, Shibasaki KI, Kato F, et al. Increased growth ability and pathogenicity of American- and Pacific-subtype zika virus (ZIKV) strains compared with a Southeast Asian-subtype ZIKV strain. PLoS Negl Trop Dis. 2019;13(6):e0007387.

Klaitong P, Smith DR. Roles of non-structural protein 4A in flavivirus infection. Viruses. 2021;13(10):2077.

Lazear HM, Diamond MS. Zika virus: new clinical syndromes and its emergence in the western hemisphere. J Virol. 2016;90(10):4864-75.

Luplertlop N, Suwanmanee S, Ampawong S, Vongpunsawad S, Poovorawan Y. In vitro study of

Zika virus infection in boar semen. Arch Virol. 2017;162(10):3209-13.

Mansuy JM, Suberbielle E, Chapuy-Regaud S, Mengelle C, Bujan L, Marchou B, et al. Zika virus in semen and spermatozoa. Lancet Infect Dis. 2016;16(10):1106-7.

Petersen LR, Jamieson DJ, Powers AM, Honein MA. Zika Virus. N Engl J Med. 2016;374(16):1552-63.

Rashid M-u, Zahedi-Amiri A, Glover KKM, Gao A, Nickol ME, Kindrachuk J, et al. Zika virus dysregulates human Sertoli cell proteins involved in spermatogenesis with little effect on tight junctions. PLoS Negl Trop Dis. 2020;14(6):e0008335.

Rastogi M, Sharma N, Singh SK. Flavivirus NS1: a multifaceted enigmatic viral protein. Virol J. 2016;13:131.

Ratchamak R, Vongpralub T, Boonkum W, Chankitisakul V. Cryopreservation and quality assessment of boar semen collected from bulk samples. Vet Med. 2019;64(5):209-16.

Sornjai W, Jaratsittisin J, Auewarakul P, Wikan N, Smith D. Analysis of Zika virus neutralizing antibodies in normal healthy Thais. Sci Rep. 2018;8(1):17193.

Wichgers Schreur PJ, van Keulen L, Anjema D, Kant J, Kortekaas J. Microencephaly in fetal piglets following in utero inoculation of Zika virus. Emerg Microbes Infect. 2018;7(1):42.

Research Articles

Dynamic Transmission of African Horse Sickness in Horse Populations during the First Epidemic in Thailand

Weesuda Phisitsak[1] Anuwat Wiratsudakul[2,3] Nuttawut Nuchprayoon[2*]

[1]Mahidol University International Demonstration School, Nakhon Pathom, 73170, Thailand
[2]Department of Clinical Sciences and Public Health, Faculty of Veterinary Science, Mahidol University, Nakhon Pathom, 73170, Thailand
[3]The Monitoring and Surveillance Center for Zoonotic Diseases in Wildlife and Exotic Animals, Faculty of Veterinary Science, Mahidol University, Nakhon Pathom 73170, Thailand

[*]Corresponding author, E-mail address: Nuttawut.nuc@mahidol.edu

Received: 17 August 2022; Revised: 23 September 2022; Accepted: 26 September 2022

Abstract

Thailand faced the first outbreak of African horse sickness (AHS) in its history in 2020. The virus firstly attacked Nakhon Ratchasima province, where a large number of naïve horses lived. In this outbreak, over four hundred horses were infected and died within three months. This study applied DengueME application to simulate how the virus spread in the horse populations with the susceptible-infectious-removed (SIR) modeling framework in horses and susceptible-infectious (SI) in vectors. The basic reproduction number (R_0), herd immunity threshold, and vaccine coverage requirement were subsequently calculated. We estimated R_0 at 3.3. With the herd immunity threshold of 69.7%, we suggested vaccinating 86.1% of horse populations to prevent future outbreaks. Our model is applicable as a baseline to test interventions such as vector control and to monitor the dynamic transmission of AHS in horse populations.

Keywords: African horse sickness, dynamic transmission, herd immunity, mathematical model

แบบจำลองพลวัตการแพร่กระจายของกาฬโรคแอฟริกาในม้า ในการระบาดครั้งแรกในประเทศไทย

วีร์สุดา พิศิฏฐศักดิ์[1] อนุวัตน์ วิรัชสุดากุล[2,3] ณัฐวุฒิ นุชประยูร[2*]

[1]โรงเรียนสาธิตนานาชาติ มหาวิทยาลัยมหิดล
[2]ภาควิชาเวชศาสตร์คลินิกและการสาธารณสุข คณะสัตวแพทยศาสตร์ มหาวิทยาลัยมหิดล
[3]ศูนย์เฝ้าระวังและติดตามโรคจาก สัตว์ป่า สัตว์ต่างถิ่นและสัตว์อพยพ คณะสัตวแพทยศาสตร์ มหาวิทยาลัยมหิดล
ถนนพุทธมณฑลสาย 4 ตำบลศาลายา อำเภอพุทธมณฑล จังหวัดนครปฐม 73170

[*]ผู้รับผิดชอบบทความ E-mail address: Nuttawut.nuc@mahidol.edu

Received: 17 August 2022; Revised: 23 September 2022; Accepted: 26 September 2022

บทคัดย่อ

ประเทศไทยได้เผชิญหน้ากับการระบาดของกาฬโรคแอฟริกาในม้าเป็นครั้งแรก ในปี พ.ศ. 2563 โดยมีรายงานการเริ่มระบาดที่จังหวัดนครราชสีมา ซึ่งเป็นจังหวัดที่มีม้าอาศัยอยู่เป็นจำนวนมาก ส่งผลให้มีม้าติดเชื้อและเสียชีวิตเป็นจำนวนมากกว่า 400 ตัว ภายในเวลา 3 เดือน ในการศึกษานี้ ผู้วิจัยได้ใช้แอพพลิเคชัน DengueME ในการจำลองสถานการณ์การแพร่ระบาดของเชื้อไวรัสผ่านแมลงพาหะด้วยแบบจำลอง susceptible-infectious-removed (SIR) ในม้า และ แบบจำลอง susceptible-infectious (SI) ในแมลงพาหะ หลังจากนั้น จึงคำนวณค่า basic reproduction number (R_0) ภูมิคุ้มกันระดับฝูง และความครอบคลุมวัคซีนที่จำเป็น ผลการคำนวณค่า R_0 ได้เท่ากับ 3.3 และค่า herd immunity threshold ได้เท่ากับ 69.7% และสัดส่วนของม้าที่ควรได้รับวัคซีนคือ 86.1% ของประชากร เพื่อป้องกันการระบาดในอนาคต แบบจำลองนี้สามารถใช้เป็นพื้นฐานในการทดสอบมาตรการอื่น เช่น การควบคุมแมลงพาหะ และใช้ในการติดตามพลวัตของการแพร่กระจายของกาฬโรคแอฟริกาในประชากรม้าได้

คำสำคัญ : กาฬโรคแอฟริกาในม้า พลวัตการแพร่ระบาด ภูมิคุ้มกันระดับฝูง แบบจำลองทางคณิตศาสตร์

Introduction

African horse sickness (AHS) is a vector-borne viral disease caused by the African horse sickness virus (AHSV). The virus belongs to the genus *Orbivirus* of the family *Reoviridae* (Dennis et al., 2019). The *Orbivirus* is also well known as a cause of bluetongue disease and epizootic hemorrhagic disease. This virus is a vector-borne disease that can be spread by biting mosquitoes, biting midges or gnats (genus *Culicoides*), and gadflies (genus *Tabanus, Haematopota, Chrysops*). Especially, the *Culicoides imicola* and *Culicoides Bolitinos* are primary vectors for AHSV (Mellor and Hamblin 2004; Slama et al., 2017).

Nine distinct serotypes of the AHSV have been recognized to date. Equids, such as horses, donkeys, mules, and zebras, are the main hosts of the virus (Spickler 2015). Zebras are generally resistant, resulting in asymptomatic infection (Porphyre and Grewar 2019). Nonetheless, serious infections mostly occur in horses, mules, and donkeys leading to high morbidity and mortality rates of 34% and 50-95 %, respectively (Spickler 2015).

The AHSV was believed to first emerge in Yemen in 1327 (Hemida et al., 2017). In 1657, the virus was documented circulating in South Africa, with a major outbreak in 1854-1855 (Dennis et al., 2019). In 1960s, animal trades and movements acted as a trigger for AHSV to spread across the Middle East, Mediterranean, Arabia, and Asia (Pakistan and India). This serotype 9 outbreak of AHSV killed approximately 300,000 equids (McKenna 2015).

According to the World Organization for Animal Health (WOAH), Thailand has been recognized as an AHS non-endemic country until 2020. AHS was first reported on March 27, 2020, in Pak Chong district, Nakhon Ratchasima province (WOAH 2020). From 24th February 2020 to 20th April 2020, Nakhon Ratchasima was ranked first with 368 infected horses. Of which, 337 horses were fatal (case-fatality rate = 91.6%) (DLD 2020). The virus was later identified as AHSV serotype 1 (Kajaysri and Toompong 2020; King et al., 2020). As it was the very first outbreak in the country, all the horses were immunologically naïve and extremely susceptible, resulting in severe clinical signs and a high mortality rate (Castillo-Olivares 2021). All forms of the clinical manifestations (cardiac, respiratory, and mixed) were detected (Kajaysri and Toompong 2020).

During the outbreak, the disease control and eradication plan had launched. The outbreak response area was determined in three zones. The infected zone, protection zone, and risk zone were the area that had a radius from the infected farm of 20 km, 50 km, and 100 km, respectively. Mostly horses in the infected and protection zones were vaccinated as much as possible to create herd immunity. The disease surveillance was carried out by clinical surveillance, vector surveillance, and active surveillance. Horse transportation was restricted. The vector control was applied by hanging up the fine mosquito net and spraying the insecticide surrounding the stable to decrease the vector population and applying the insect repellent on the horses (DLD 2020; Ketusing 2020).

Mathematical modeling is an epidemiological tool used to describe the dynamic transmission of infectious diseases (Wiratsudakul et al., 2018). These models are basically built based on relevant epidemiology concepts (Huppert and Katriel 2013). The compartmental model has been widely used to simulate different infectious diseases due to its simplicity and ability to produce results in a timely fashion. Susceptible-Infectious-Recovered (SIR) is a compartmental model that was first proposed by Kermack and McKendrick (Doungmo Goufo et al., 2014). The model has been used for diseases that spread quickly with a short incubation period, such as Avian Influenza (Guan et al., 2007), COVID-19 (Cooper et al., 2020), and Chickenpox (Devi and Devachoudhury 2018). In the case of vector-borne diseases, additional compartments for the vectors are added to the classical SIR model (Wiratsudakul et al., 2018). The SIR-SI model is one of the widely used models for such diseases. The model has been used to describe the spread of Zika virus (Boreta et al., 2017), Dengue (Pandey et al., 2013), and Malaria (Putri et al., 2014). In the study of AHS, some mathematical models have already been developed (Lord et al., 1998; Backer and Nodelijk 2011). However, none was specifically tailored to the situations in Thailand.

This study, therefore, aimed to describe the dynamic transmission of AHSV in horse populations in Nakhon Ratchasima and further recommend the vaccine coverage requirement for the effective control of the disease in Thailand.

Materials and Methods

Data Retrieval

We retrieved the daily number of horses that were infected and died from the AHSV infections from the Thai Society of Equine Practitioners and the Department of Livestock Development, Thailand. The total number of horses was 1,835 horses from 117 horse farms in every district of Nakhon Ratchasima province, Thailand. This province contains 32 districts. Most horses were lived in Pak Chong district (1327/1835) and Muang district (390/1835). Most horses in Muang district were racehorses; meanwhile, Pak Chong district had many types of horses for several purposes i.e. competition, pleasure riding, western riding, showing, etc. Neither human nor animal ethical approval was required as only the secondary data was used; moreover, no humans and animals were involved in the study.

Estimation of vector population

Due to the data on the biting midges in Nakhon Ratchasima is not available, we then extrapolated the number of biting midges from a previous study. Thepparat et al., (2012) reported that the density of biting midges was 40.5 midges/km^2 in the area of Parai subdistrict, Arunyaprathet district, Sakaew province, Thailand. The size of Nakhon Ratchasima compared to Parai subdistrict is shown in Figure 1. The area of Nakhon Ratchasima was 12,495.13 km^2. Hence, the number of the biting midges in Nakhon Ratchasima was then estimated at 506,473 midges.

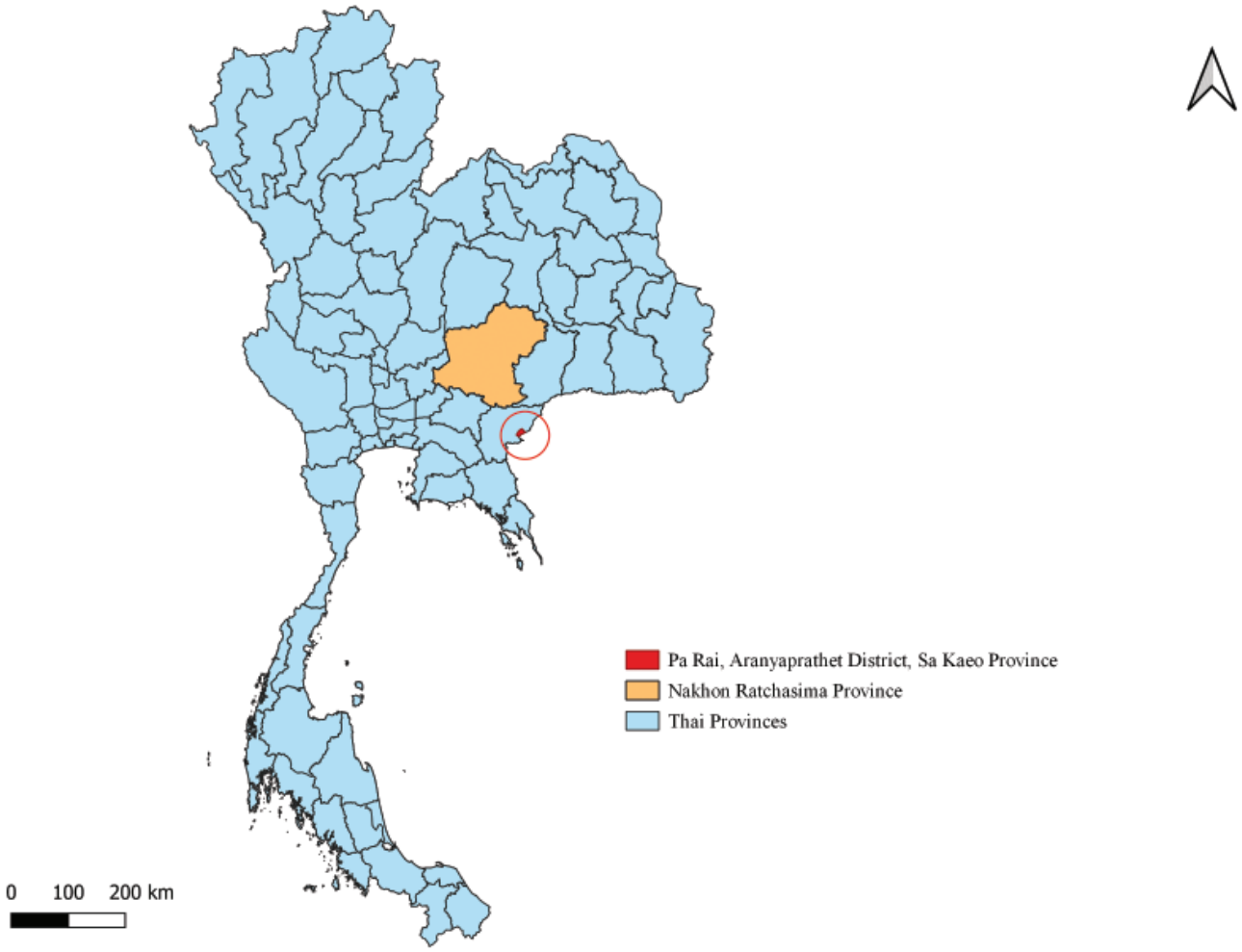

Figure 1. Geographical comparison between Parai subdistrict (red area) and Nakhon Ratchasima province (orange area) that the density of the biting midges was estimated.

Dynamic transmission of AHS in Nakhon Ratchasima province

An SIR-SI compartmental model was constructed to simulate how AHSV spread between horse and vector populations (Figure 2). The duration of the model was designed as 120 days. The dynamic transmission of the virus followed a set of differential equations shown in Eq 1. All parameters used in the equation were defined in Table 1. For the number of infected vectors during time t ($I_v(t)$) and the biting rates (α), we fitted the SIR-SI model with the given observed data until we got the values that reflected the field data. The software DengueMe (Federal University of Ouro Preto, Ouro Preto, Brazil, and National Institute for Space Research, São José dos Campos, Brazil) was used throughout the simulation.

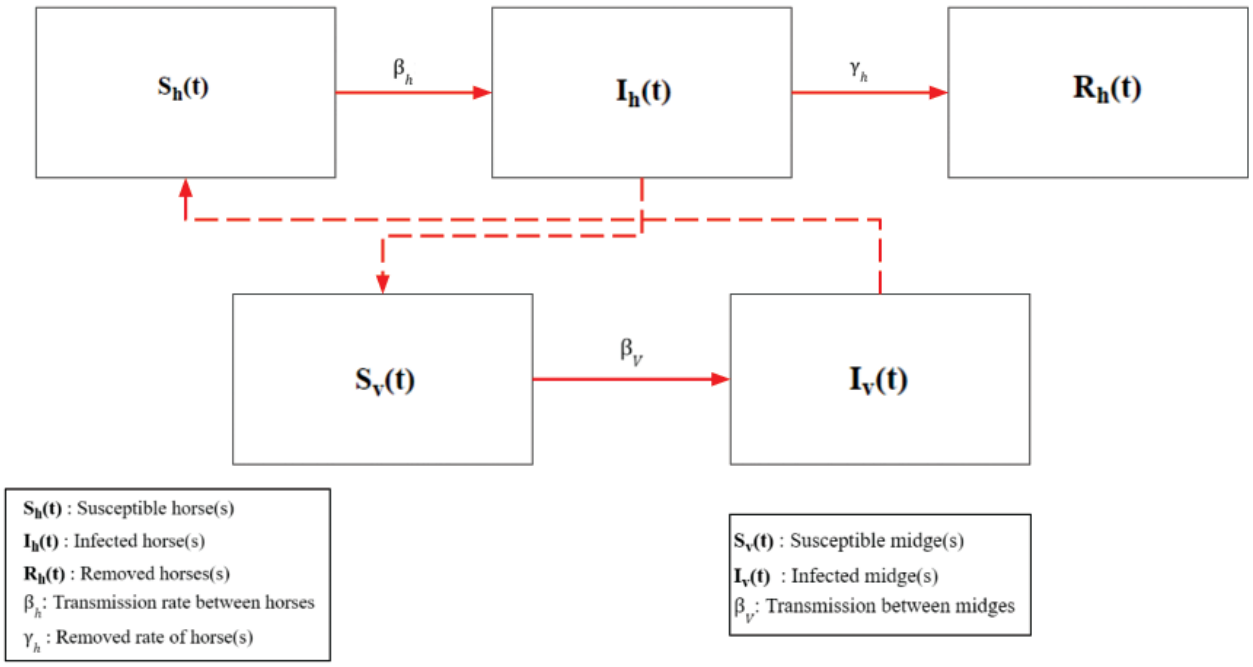

Figure 2. Conceptual framework of AHS model in Nakhon Ratchasima province.

Table 1. Model parameters for the AHS transmission model in Nakhon Ratchasima province.

Parameter	Definition	Values	References
$S_h(t)$	Numbers of susceptible hosts during time *t*	1,834 horses	Field data
$I_h(t)$	Numbers of infected hosts during time *t*	1 horse	Initial condition
$R_h(t)$	Numbers of removed hosts during time *t*	0 horse	Initial condition
$S_v(t)$	Numbers of susceptible vectors during time *t*	506,472 biting midges	Calculated from Thepparat et al., (2012)
$I_v(t)$	Numbers of infected vectors during time *t*	1 biting midges	Estimated from epidemic curve
α	The biting rates (Assumed constant and equal for all the hosts)	0.08 (1 vector/day)	Estimated from epidemic curve

Table 1. Model parameters for the AHS transmission model in Nakhon Ratchasima province. (Cont.)

Parameter	Definition	Values	References
β_h	Transmission probability from vectors to hosts	0.770	Backer & Nodelijk (2011)
β_v	Transmission probability from hosts to vectors	0.040	Backer & Nodelijk (2011)
γ_h	The rate at which the infected hosts are removed from the population	0.230	Backer & Nodelijk (2011)

Horses (Host) (Eq 1.)

$$S_h(t) = -\alpha\beta_h S_h(t) I_v(t)$$

$$I_h(t) = \alpha\beta_h S_h(t) I_v(t) - \gamma_h I_h(t)$$

$$R_h(t) = \gamma_h I_h(t)$$

Midges (Vector)

$$S_v(t) = -\alpha\beta_v I_h(t) S_v(t)$$

$$I_v(t) = \alpha\beta_v I_h(t) S_v(t)$$

, where the initial conditions were set for both host (horse) and vector (midges) parts as demonstrated in Table 1.

Estimation of the basic reproduction number

The transmission and recovery rates were used for calculating the basic reproduction number (R_0). The formula for calculating R_0 was described by Gubbins (2019) as shown in Eq 2.

$$R_0 = \sqrt{\frac{ba}{\gamma+\mu} \times \frac{\beta m a}{r_I}} \quad \text{(Eq 2.)}$$

In addition, all parameters for calculating R_0 are noted in Table 2. Once the midge has its bloodmeal on the infected horses, a midge persists infected and contagious until the virus becomes inactivated or the vector dies out. In the mathematical term, it can be expressed as $1/(\gamma + \mu)$, a period in which the virus lasts on average days, where γ is the virus inactivation rate and μ is the mortality rate of midges. Concurrently, a midge can bite the susceptible hosts times per day (*a* is the reciprocal of the time interval between the blood meals), and proportion of these bites, noted as *b* (probability of transmission from midges to horses), is 0.770. To calculate *a*, we did the reciprocal of blood feeding interval of midges, 7.5, getting 1/7.5. This will result in newly infected horses. After horses are infected, the horses will continue to be contagious for its infectious phase, which typically lasts $1/r_I$ days. According to Backer & Nodelijk (2011), horses remain infectious for 4.4 days. During this time, the midges will bite the horses *m* x *a* times per day (*m* is the ratio of

vector to hosts), 276 midges per 1 horse. Along with the proportion, β (probability of transmission from horse to midge) is responsible for the rise of newly infected midges.

Herd immunity threshold and vaccine coverage requirement

Herd immunity threshold was calculated from the R_0 (Herd immunity = $1\frac{1}{R_0}$) (Lahariya 2016). The efficacy of the AHS vaccine was up to 81% (Dennis et al., 2019). Vaccine coverage requirement was then calculated from a proportion of the herd immunity and the vaccine efficacy ($Vc = \frac{\text{Herd immunity (qc)}}{\text{vaccine efficacy (E)}}$) (MacIntyre et al., 2021).

Table 2. Model parameters for calculating R_0.

Parameter	Definition	Values	References
b	Probability of transmission from midge to horse	0.77	Backer & Nodelijk (2011)
a	Reciprocal of time interval between the blood meals	$\frac{1}{7.5}$	Backer & Nodelijk (2011)
γ + μ	γ is the virus inactivation rate μ is the midge's mortality rate	16	Backer & Nodelijk (2011)
β	Probability of transmission from horse to midge	0.04	Backer & Nodelijk (2011)
m	Midge to horse ratio (N/H; N and H are the number of midges and horses, respectively)	276	Calculated from given field data
$\frac{1}{r_I}$	Average infection period dying hosts rate (days)	$\frac{1}{4.4}$	Backer & Nodelijk (2011)

Results

Observed AHS outbreaks in Nakhon Ratchasima province

The first group of infected horses was detected in Pak Chong district and then rapidly widespread to a nearby area. Overall, there were 56 farms in Nakhon Ratchasima confronted with the AHSV from 24th February 2020 to 20th April 2020. The number of sick and dead horses was 368 and 337 horses, respectively (DLD 2020). These cases were positively confirmed with RT-PCR (Bunpapong et al., 2021). The number of sick horses was used as baseline data to plot the epidemic curve, as shown in Figure 3.

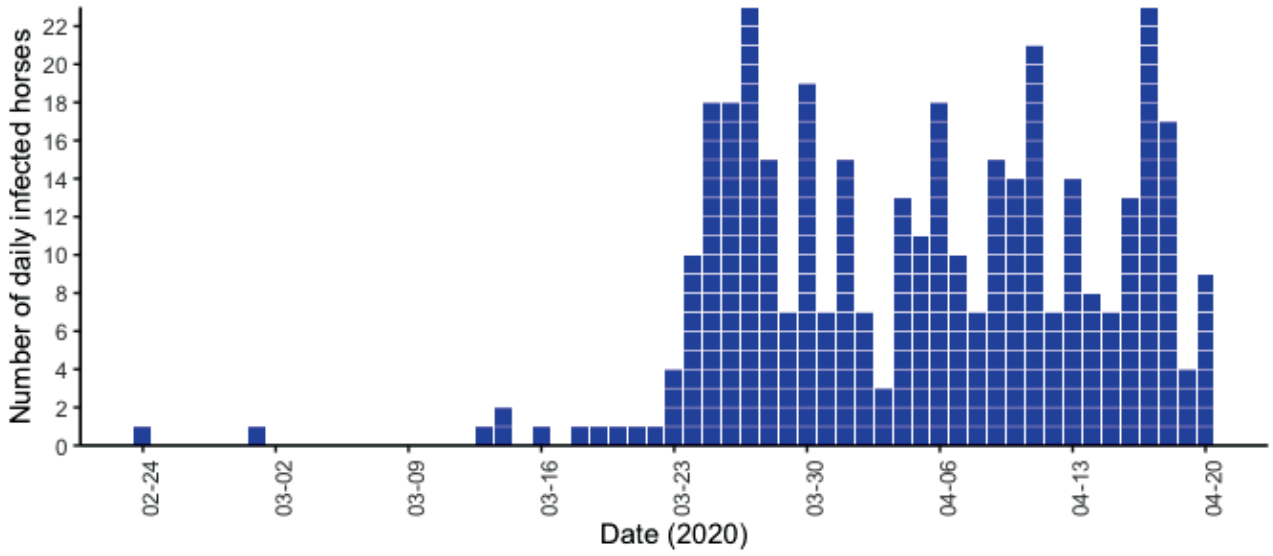

Figure 3. Epidemic curve of daily infected horses in Nakhon Ratchasima province during 24th February to 20th April 2020 (Data source: DLD 2020).

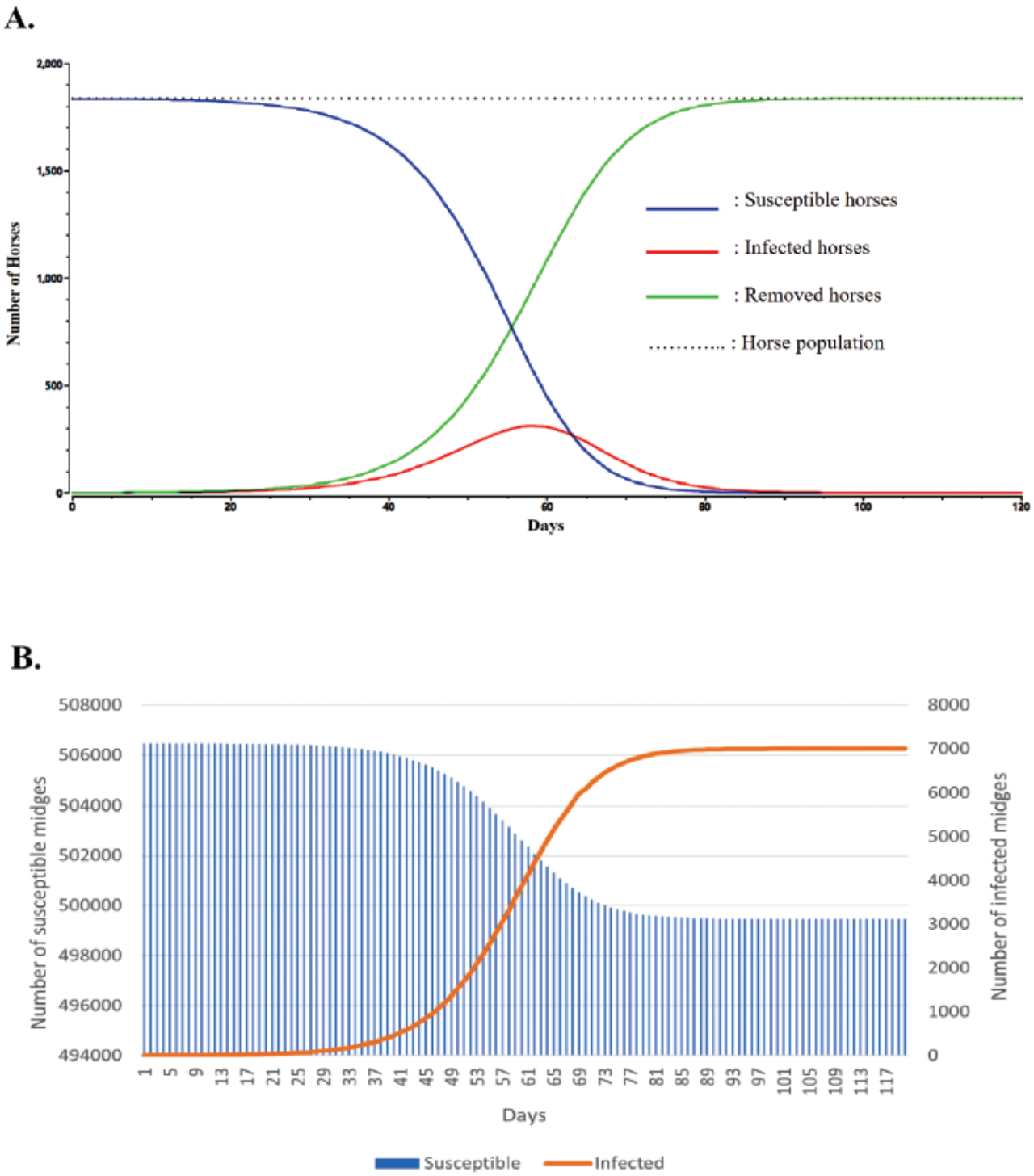

Figure 4. Dynamic transmission of AHSV in Nakhon Ratchasima province. A. Results in host populations B. Results in vector populations.

Dynamic transmission of AHSV in Nakhon Ratchasima province

In the host populations (Figure 4A), the number of infected horses peaked on day 59 and then gradually decreased later. The number of cases declined to zero on day 85. In the vector populations (Figure 4B), the number of susceptible midges was inversely proportional to the number of infected midges as there was a decline in the number of susceptible midges along the course of the outbreaks while the number of infected midges inclined. Throughout the studies, there was a significant change in the number of infected and susceptible midges. The number of infected midges started rising exponentially from 106 midges to 6,925 midges from day 28 until day 83. Later, the infectious rate of midges drops rapidly. Once, the infected midgesí population reached 6,999 midges on day 104, it remained nearly unchanged. On day 116, the number of infected midges reached its peak and threshold at 7,000, and there were no shifts afterward. On the other hand, the trend of susceptible midges went directly opposite to infected midges.

Values of basic reproduction number, herd immunity threshold, and vaccine coverage requirement

Based on our calculation, we estimated the values of basic reproduction number, herd immunity threshold, and vaccine coverage requirement at 3.3, 69.7%, and 86.1%, respectively.

Discussion

The present study used a mathematical model to demonstrate how the AHSV spread in horse populations in a province where the virus firstly emerged in Thailand. The field data were collected during the epidemic and used to estimate the disease transmission parameters. The herd immunity threshold and the vaccine coverage requirement were then suggested.

This study used the SIR-SI model for mathematical modeling. We omitted the E compartment as most infected horses in the actual outbreaks died relatively quickly, within a few days after showing clinical signs. Hence, such a short incubation period may be insufficient to transmit the disease from the asymptomatic infected horses to the susceptible ones.

Based on the epidemic curve (Figure 3), we found that the virus spread in the horse population like wildfire. Given that the AHS attacked Thailand for the first time, all affected horses were completely susceptible. Our model assumed that the population was homogeneous; however, there were many categories of horses in Nakhon Ratchasima province, which led to the heterogenicity of the population.

During the study period, the mortality rate of horses was observed at 91.6% (337/368). Our finding is in line with a previous study in the Western Cape province, South Africa when the AHSV type 1 was first notified in 2004 (Venter et al., 2006). In that outbreak, the mortality rate was recorded at more than 90% (Thompson et al., 2012). This is concrete evidence addressing the highly infectious

characteristic of AHSV, especially in territories where the virus firstly hit.

As AHS is a vector-borne disease, the dynamic transmission greatly depends on how the virus spreads in both host and vector populations. Our model suggested that the number of infected horses peaked on day 59 (Figure 4A), and the number of infected midges was raised up to almost at the peak level on day 83 (Figure 4B). Our peak of the infected horses was delayed than a previous study conducted in South Africa. Their epidemic curve revealed that the peak number of infected horses was evident in the fourth week (Grewar et al., 2013). The soil moisture is an important factor for midges to develop their larva development, so the climate and weather are necessary factors affect to the number of midges (Diarra et al., 2018). The temperature during summer in Nakhon Ratchasima is between 21-37^{o}C, whereas, in the Western Cape, South Africa, it is between 15-27^{o}C. Hence, the hotter temperature in Nakhon Ratchasima might decrease the density of midges and delay the transmission rate of AHSV.

Once most of the horses are infected, other horses in the area are protected by herd immunity. A large new outbreak will not likely occur in the area. However, the travel distance of midges may vary from 40-700 km to the prevailing wind (Sellers et al., 1977). The epidemic can rapidly expand to surrounding areas where fully susceptible horses are raised. In Thailand, for example, the AHS occupied 18.18% of provinces (14/77) in the country within only 6 months (Yothakol 2019). Interestingly, the epidemic occurred in Nakhon Ratchasima, Prachuap Khirikhan, and Chonburi province, respectively, which has no adjoined border (DLD 2020). The intermittent distribution pattern of disease might come from the transportation of infected horses by illegal animal movement or feed/hay truck movement from the epidemic to non-epidemic area (Ketusing 2020). Moreover, the infected midges can also be hidden within the vehicle and then spread into the new area.

Early detection and prompt response to the outbreak are crucially important. In 1989, the outbreak of AHS in Southern Portugal was rapidly eradicated within 13 weeks with an effective vaccination policy, restriction of animal movement, and eradication campaign on infected horses (Portas et al., 1999). Besides, vector control programs should be urgently implemented in the non-outbreak areas once the virus is detected in the vicinity.

The basic reproduction number is an important epidemiological parameter indicating how fast a certain disease spreads (Lord et al., 1996). In this study, we estimated this value at 3.3. Our result aligns with a previous study in which the R0 was found at 2.6-8.0 (Backer and Nodelijk 2011). Indeed, the R0 of AHS was relatively high compared to other infectious diseases in horses, such as equine infectious anemia (R_0 = 0.18-1.9) (Schwartz and Smith 2014), equine influenza (R_0 = 2-5) (Satou and Nishiura 2006) and equine herpes virus type 1 (R0 = 2.94-10.25) (Meade 2012). AHS thus spread more rapidly. Therefore, the relevant control efforts must be

rigorously implemented once the virus is detected.

Vaccination is an effective tool used to combat AHS. Selection of vaccine had to be matched with the serotype of the outbreak situation. In this very first AHS outbreak in Thailand, the polyvalent vaccine (serotypes 1, 3, and 4) was employed in which the vaccine efficiency was estimated at up to 81% (Dennis et al., 2019). That could provide the herd immunity threshold estimated to be around 69.7%. In a previous study, the protective herd immunity for AHS was estimated at 50% if 75% of the entire horses were vaccinated (Lord et al., 1997). These high herd immunity values reflect the high proportion of immunized horses. We recommended vaccinating at least 86.1% of the horse population. The eradication program in Portugal in 1999 vaccinated all horses in the country (Portas et al., 1999).

We used data from 2020, which was 2 years ago. The first vaccination campaign in 2020 was accomplished, in which 86.7% of total horses within Nakhon Ratchasima province (1,219 of 1,405) were vaccinated. This is agreed with our recommended number of vaccinations at least 86.1%. The latest case of AHS in Thailand was reported on 10th September 2020 in zebra and there was no further report of infected horses until September 2022 (Ketusing 2020). This implied that the national eradication plan, including disease surveillance, vaccination campaign, vector control, and movement control, was effective in controlling the epidemic and reducing the number of infected and dead horses.

In this study, we faced some potential limitations. First, the follow-up data collection from vaccinated and un-vaccinated horses in Thailand was insufficient to calculate the vaccine efficacy from an actual outbreak. We hence used the value estimated from a previous study (Dennis et al., 2019). In future studies, the number of sick animals should be recorded from both vaccinated and un-vaccinated horses after implementing a mass vaccination campaign. Such data is very useful for calculating vaccine efficiency from a particular outbreak. A future field study on estimating the number of midges is recommended to get the baseline data. Second, our model did not include the mortality rate of the vectors in each phase. Moreover, the transmission rate from midges to host did not describe all the biting rate, pathogen transmission efficiencies, daily survival rate of vectors, and duration of the extrinsic incubation period. Third, our model focused on only one province. Indeed, the virus had spread already to different provinces across Thailand. A nationwide study is suggested. Nevertheless, the modeling framework proposed here is extendable once more data is available.

Conclusion

Based on our model, we recommend vaccinating at least 86.1% of the horse population to prevent the upcoming AHS outbreaks. This model is applicable as a baseline to test interventions such as vector control and to monitor the dynamic transmission of AHS in the future.

Acknowledgements

The field data of AHS situation in Thailand was the result of collaboration between Department of Livestock Development and The Thai Society of Equine Practitioners. This study received no specific funding.

References

Backer JA, Nodelijk G. Transmission and control of African horse sickness in the Netherlands: a model analysis. PLoS One. 2011;6(8):1-12.

Boret SEB, Escalante R, Villasana M. Mathematical modelling of zika virus in Brazil. arXiv:1708. 01280.2017:1-26.

Bunpapong N, Charoenkul K, Nasamran C, Chamsai E, Udom K, Boonyapisitsopa S, et al. African horse sickness virus serotype 1 on horse farm, Thailand, 2020. Emerg Infect Dis. 2021;27(8):2208-11.

Castillo-Olivares J. African horse sickness in Thailand: Challenges of controlling an outbreak by vaccination. Equine Vet J. 2021;53(1):9-14.

Cooper I, Mondal A, Antonopoulos CG. A SIR model assumption for the spread of COVID-19 in different communities. Chaos Solitons Fractals. 2020;139: 1-14.

Dennis SJ, Meyers AE, Hitzeroth II, Rybicki EP. African horse sickness: a review of current understanding and vaccine development. Viruses. 2019;11(9):1-24.

Devi R, Devachoudhury BK. SIR model for transmission of chickenpox in Kamrup Metro District of Assam. Int J Eng Sci Technol. 2018;8(2S):98-102.

Diarra M, Fall M, Fall AG, Diop A, Lancelot R, Seck MT, et al. Spatial distribution modelling of *Culicoides* (Diptera: Ceratopogonidae) biting midges, potential vectors of African horse sickness and bluetongue viruses in Senegal. Parasit Vectors. 2018;11(1):341.

DLD. African horse sickness (AHS) in Thailand [internet]. Department of Livestock Development. 2020 [cited 2022 Sep 21]. Available from: https://rr-asia.woah.org/wp-content/uploads/2020/06/1-update-on-situation-in-thailand.pdf.

Doungmo Goufo EF, Oukouomi Noutchie SC, Mugisha S. A fractional SEIR epidemic model for spatial and temporal spread of measles in metapopulations. Abstr Appl Anal. 2014;2014:1-6.

Grewar JD, Weyer CT, Guthrie AJ, Koen P, Davey S, Quan M, et al. The 2011 outbreak of African horse sickness in the African horse sickness controlled area in South Africa. J S Afr Vet Assoc. 2013;84(1): 1-7.

Guan Y, Chen H, Li K, Riley S, Leung G, Webster R, et al. A model to control the epidemic of H5N1 influenza at the source. BMC Infect Dis. 2007;7:1-8.

Gubbins S. Using the basic reproduction number to assess the risk of transmission of lumpy skin disease virus by biting insects. Transbound Emerg Dis. 2019;66(5):1873-83.

Hemida M, Alhammadi M, Daleb A, Alnaeem A. Molecular and serological surveillance of African horse sickness virus in Eastern and Central Saudi Arabia. Rev Sci Tech Off Int Epiz. 2017;36(3):1-22.

Huppert A, Katriel G. Mathematical modelling and prediction in infectious disease epidemiology. Clin Microbiol Infect. 2013;19(11):999-1005.

Kajaysri J, Toompong J. African horse sickness: the emerging infectious diseases in thailand. APHEIT Journal. 2020;1:1-8.

Ketusing N. African horse sickness in Thailand [internet]. Division of International Livestock Cooperation. 2020 [cited 2022 Sep 21]. Available from: https://rr-asia.woah.org/wp-content/uploads/2020/11/thailand_ahs-situation_10nov2020.pdf.

King S, Rajko-Nenow P, Ashby M, Frost L, Carpenter S, Batten C. Outbreak of African horse sickness in Thailand, 2020. Transbound Emerg Dis. 2020:1-4.

Lahariya C. Vaccine epidemiology: A review. J Family Med Prim Care. 2016;5(1):7-15.

Lord CC, Woolhouse MEJ, Heesterbeek JAP, Mellor PS. Vector-borne diseases and the basic reproduction number: a case study of African horse sickness. Med Vet Entomol. 1996;10:19-28.

Lord CC, Woolhouse MEJ, Mellor PS. Simulation studies of vaccination strategies in African horse sickness. Vaccine. 1997;15(5):519-24.

Lord CC, Woolhouse MEJ, Mellor PS. Simulation studies of African horse sickness in Spain. In: Mellor PS, Baylis M, Hamblin C, Mertens PPC, Calisher CH, editors. African horse sickness. Vienna: Springer; 1998. p. 103-11.

MacIntyre CR, Costantino V, Trent M. Modelling of COVID-19 vaccination strategies and herd immunity, in scenarios of limited and full vaccine supply in NSW, Australia. Vaccine. 2022;40:2506-13.

McKenna TSC. Overview of African horse sickness [internet]. MSD Veterinary Manual. 2015 [cited 2022 Aug 16]. Available from: https://www.msdvetmanual.com/generalized-conditions/african-horse-sickness/overview-of-african-horse-sickness.

Meade BJ. The transmission dynamics of equine herpes virus type 1 (EHV-1) infection in outbreaks characterized predonminately by neurological or respiratory illness. Lexington: University of Kentucky; 2012.

Mellor PS, Hamblin C. African horse sickness. Vet Res. 2004;35(4):445-66.

Pandey A, Mubayi A, Medlock J. Comparing vector-host and SIR models for dengue transmission. Math Biosci. 2013;246(2):252-9.

Porphyre T, Grewar JD. Assessing the potential of plains zebra to maintain African horse sickness in the Western Cape Province, South Africa. PLoS One. 2019;14(10):1-24.

Portas M, Boinas FS, Oliveira J, Sousa E, Rawlings P. African horse sickness in Portugal: a successful eradication programme. Epidemiol Infect. 1999; 123:337-46.

Putri RG, Jaharuddin, Bakhtiar T. Sirs-Si Model of malaria disease with application of vaccines, anti-malarial drugs, and spraying. IOSR J Math. 2014; 10(5):66-72.

Satou K, Nishiura H. Basic reproduction number for equine-2 influenza virus A (H3N8) epidemic in racehorse facilities in Japan, 1971. J Equine Vet Sci. 2006;26(7):310-6.

Schwartz EJ, Smith RJ. Identifying the conditions under which antibodies protect against Infection by equine infectious anemia virus. Vaccines (Basel). 2014; 2(2):397-421.

Sellers RF, Pedgley DE, Tucker MR. Possible spread of African horse sickness on the wind. J Hyg. 1977; 79:279-98.

Slama D, Babba H, Chaker E. *Culicoides* spp. (Diptera: Ceratopogonidae) in Tunisia. In: Shields VDC, editor. Biological Control of Pest and Vector Insects. *Culicoides* spp. (Diptera: Ceratopogonidae) in Tunisia: IntechOpen; 2017. p. 213-29.

Spickler AR. 2015. African horse sickness. The Center for Food Security & Public Health. p. 1-6.

Thepparat A, Tsuruishi T, Ketavan C. Species Diversity and Abundance of *Culicoides* (Diptera : Ceratopogonidae) in Sakaew Province. Ramkhamhaeng University Journal of Research. 2012;15(2):65-80.

Thompson GM, Jess S, Murchie AK. A review of African horse sickness and its implications for Ireland. Ir Vet J. 2012;65(9):1-8.

Venter GJ, Koekemoer JJO, Paweska JT. Investigations on outbreaks of African horse sickness in the surveillance zone in South Africa. Rev Sci Tech Off Int Epiz. 2006;25(3):1097-109.

Wiratsudakul A, Suparit P, Modchang C. Dynamics of Zika virus outbreaks: an overview of mathematical modeling approaches. PeerJ. 2018;6:1-30.

WOAH. African horse sickness [internet]. WOAH 2020 [cited 2022 Aug 16]. Available from: https://www.woah.org/en/disease/african-horse-sickness/.

Yothakol C. Protocol for horse transportation after vaccination (in Thai language) [internet]. Department of Livestock Development. 2019 [cited 2022 Aug 16]. Available from: http://dcontrol.dld.go.th/webnew/index.php/th/news-menu-2/african-horse-sickness/4110-african-horse-sickness-2563.

Mahidol University
Faculty of Veterinary Science

Excellence in Research with Social and Global Impact

Our research expertise

- Zoonosis
- Wildlife Research
- Veterinary Clinical Research
- Vector-borne Infectious Diseases
- Proteomics and Biomedical Science
- Stem Cells and Animal Biotechnology
- Animal Infectious Disease Surveillance
- Veterinary Pharmacology and Herbal Medicine
- Veterinary Epidemiology and Mathematical Modellings

For more information please contact www.vs.mahidol.ac.th or call 02-441-5242 /MUVetSci

Mahidol University
Faculty of Veterinary Science

Study Veterinary Science at Thailand's Top University*

*Ranked by:
QS World University Rankings by Subject 2019
Times Higher Education Asia University Rankings 2019
The CWTS Leiden Ranking 2019
2019 Asian University Ranking by UniRank (4icu.org)
UI Green Metric World University Rankings 2018

Undergraduate Programme

Doctor of Veterinary Medicine (6 years programme)

Postgraduate Programme

Doctor of Philosophy (PhD) in Veterinary Science (International Programme)

- Production Medicine
- Companion Animal Medicine
- Pathology
- Epidemiology

Master of Science (MSc) in Veterinary Biomedical Science (International Programme)

- Veterinary Diagnostic Sciences
- Applied Veterinary Biomedical Sciences and Veterinary Public Health
- Zoo Animal and Wildlife Health Management

Graduate Diploma (Grad Dip) (International Programme)

- Clinical Veterinary Science

For more information please contact www.vs.mahidol.ac.th or call 02-441-5248 /MUVetSci